Quaternary Science Reviews 30 (2011) 176–191

Contents lists available at ScienceDirect

Quaternary Science Reviews

journal homepage: www.elsevier.com/locate/quascirev

Holocene temperature variations at a high-altitude site in the Eastern Alps: a chironomid record from Schwarzsee ob Sölden, Austria

Elena A. Ilyashuk[a,b,*], Karin A. Koinig[a], Oliver Heiri[c], Boris P. Ilyashuk[b,c], Roland Psenner[a]

[a] Institute of Ecology, University of Innsbruck, Technikerstraße 25, A-6020 Innsbruck, Austria
[b] Institute of North Industrial Ecology Problems, Kola Science Centre, Russian Academy of Sciences, 14 Fersman St., Apatity, Murmansk Reg., 184209, Russia
[c] Institute of Environmental Biology, Palaeoecology, Laboratory of Palaeobotany and Palynology, Utrecht University, Budapestlaan 4, NL-3584 CD Utrecht, The Netherlands

ARTICLE INFO

Article history:
Received 15 February 2010
Received in revised form
20 September 2010
Accepted 13 October 2010

ABSTRACT

Few well-dated, quantitative Holocene temperature reconstructions exist from high-altitude sites in the Central Eastern Alps. Here, we present a chironomid-based quantitative reconstruction of mean July air temperatures (T_{July}) throughout the Holocene for a remote high-mountain lake, Schwarzsee ob Sölden, situated above the treeline at 2796 m a.s.l. in the Austrian Alps. Applying a chironomid-temperature inference model developed from lakes of the Alpine region to a high-resolution chironomid record from the lake provides evidence for early Holocene (ca 10000–8600 cal yr BP) T_{July} of up to 8.5 °C, i.e. >4 °C above the modern (1977–2006) mean July temperature. The reconstruction reveals the so-called '8.2-ka cold event' centered at ca 8250–8000 cal yr BP with temperatures ca 3 °C below the early-Holocene thermal maximum. Rather warm (ca 6 °C) and productive conditions prevailed during ca 7900–4500 cal yr BP. The chironomid record suggests a climate transition between ca 5200 and 4500 cal yr BP to cooler T_{July}. A distinct cooling trend is evident from ca 4500 until ca 2500 cal yr BP. Thereafter, the study site experienced its coldest conditions (around 4 °C or less) throughout the rest of the Holocene, with the exception of the warming trend during the late 20th century. Beside other factors, the Northern Hemisphere summer insolation seems to be the major driving force for the long-term trends in T_{July} at high altitudes in the Eastern Alps. Due to the extreme location of the lake and the limited temperature range represented by the applied calibration data set, the chironomid-based temperature reconstruction fails to track phases of the late-Holocene climatic history with T_{July} cooler than 4 °C. Further chironomid-based palaeoclimate model and down-core studies are required to address this problem, provide more realistic T_{July} estimates from undisturbed high-altitude lakes in the Alps, and extract a reliable regional temperature signal.

1. Introduction

The European Alps, one of the great mountain systems of Europe, form a climatic barrier between Atlantic, continental and Mediterranean climate, and, therefore, have a major significance in determining European climate dynamics (Beniston and Jungo, 2002). In the Alps, the temperature increases observed during the past several decades are two to three times higher than global linear warming (Beniston, 2006; Auer et al., 2007). For each 1 °C of temperature increase, the duration of snow cover is expected to decline by several weeks at mid-elevations in the European Alps (Bates et al., 2008). Ice-cover and water temperatures of alpine lakes are also controlled by air temperatures, and so are very susceptible to shifts in climate (Thompson et al., 2005). On a local scale factors such as wind exposure, shading etc. may determine the sensitivity of an alpine lake towards external influences. Generally, however, alpine lakes are recognized as ideal indicators of global climate change (Battarbee, 2000; Adrian et al., 2009).

Global warming has vital ecological and economic consequences and is one of the greatest threats the planet is facing today. Reconstructions of temperature changes over a few hundred or thousand years, based on proxy data providing a record of temperature over long periods of time, are necessary to quantify past climatic variability on a longer temporal scale and to provide important background knowledge for a better understanding of the recent warming process, including its timing, intensity, and causes (Crowley, 1996). The high topographic complexity of the Alpine region is the origin of important climate differences that characterize the different areas of the Alps. Therefore, one of the main aims of Alpine palaeoclimatology today is not only to quantify past

* Corresponding author. Institute of Ecology, University of Innsbruck, Technikerstraße 25, A-6020 Innsbruck, Austria.
E-mail address: elena.ilyashuk@uibk.ac.at (E.A. Ilyashuk).

0277-3791 © 2010 Elsevier Ltd. Open access under CC BY-NC-ND license.
doi:10.1016/j.quascirev.2010.10.008

climate, but also to develop a dense network of palaeoclimatic sites to advance our knowledge about the controlling mechanisms and the temporal and spatial patterns of climatic and environmental changes within the Alpine region.

Subfossil remains of chironomid larvae (Diptera: Chironomidae) from lake sediments are widely recognized as particularly useful palaeotemperature indicators (Walker, 1995; Battarbee, 2000). It has been shown that the relationship between summer air temperature and the modern-day distribution of chironomids can be successfully used for the reconstruction of past summer temperature changes from lacustrine sediment records in the Alpine region (Heiri et al., 2003; Larocque and Finsinger, 2008; Ilyashuk et al., 2009) and other parts of Europe (Langdon et al., 2004; Ilyashuk et al., 2005; Velle et al., 2005; Heiri et al., 2007a). Today chironomid analysis of sediment records is widely used in palaeoecology and palaeoclimatology within multi-proxy projects.

At present, there exists a large set of palaeoclimatic data from the Central and Western Alps, based on different proxies, but only a fragmentary record from the Eastern Alps. As regards the Austrian Alps, quantitative palaeoclimatic records are still sparse. Recently, Huber et al. (2010) have reconstructed summer water temperatures for the time window of ca 19–13 cal ka BP based on diatom assemblages from a lake in Carinthia, southern Austria. Chrysophyte cyst and diatom records from a lake in the Niedere Tauern, central Austria, were used to infer spring and autumn air temperature anomalies for the past four millennia (Schmidt et al., 2007). Geochemical, mineralogical and biological proxies were used for climate inferences in the Niedere Tauern throughout the time window of 12–4 cal ka BP (Schmidt et al., 2006). Stalagmites from Katerloch Cave located in Styria, southeast Austria, have shown evidence of prominent climate changes at the south-eastern fringe of the Alps in the early Holocene (Boch et al., 2009). The oxygen isotope composition of a stalagmite from the high-alpine Spannagel Cave located in Zillertal Alps, Tyrol, western Austria, provided a high-resolution reconstruction of annual temperature changes during the past 9000 years (Vollweiler et al., 2006; Mangini et al., 2007). A dendrochronological treeline record for the last 9000 years is available from the timberline ecotone in the Kauner valley in the Ötztal Alps, Tyrol, western Austria (Nicolussi et al., 2005). There are also tree-ring based palaeoclimate reconstructions providing evidence of millennium-long summer temperature variations in the Austrian Alps (Büntgen et al., 2005; Corona et al., 2008). A 9111 year long Eastern Alpine Conifer Chronology based on the analysis of dead wood samples from sites above 2000 m a.s.l., which can be used as a dating base for regional environmental studies, has been recently established by Nicolussi et al. (2009).

With respect to chironomid-based inferences, a number of quantitative temperature reconstructions at centennial and millennial time-scales have recently been implemented in the Swiss Alps (Heiri et al., 2003; Heiri and Lotter, 2005; von Gunten et al., 2008; Ilyashuk et al., 2009; Larocque et al., 2009), the Italian Alps (Heiri et al., 2007b; Larocque and Finsinger, 2008), and the French Alps (Millet et al., 2009). However, no quantitative chironomid-based inferences of climatic changes have been available from the Austrian Alps.

Here we present results of the first palaeoecological study from the Austrian Alps using chironomids in an attempt to quantify past temperature variability in the region during the Holocene. This is the highest site studied hitherto in the European Alps from which temperatures were reconstructed based on chironomid record. This research is part of a multi-proxy palaeoecological investigation including diatoms, pollen, geochemistry, mineralogy, grain size, and palaeomagnetic analyses of the sediment records from a remote high-alpine lake located in the Tyrolean Alps. Only subfossil chironomids as a biological proxy for palaeoclimate are considered in this paper. In addition, we assessed the modern distribution of benthic macroinvertebrates, mainly of chironomid larvae, along a transect across the deepest point in the lake to delineate the habitat preferences of resident larvae in the modern ecosystem. The obtained information contributes to a better palaeoenvironmental interpretation of changes in the subfossil chironomid record through time, and helps to understand taphonomic effects on subfossil chironomids in the lake.

2. Study site

Schwarzsee ob Sölden (SOS; 46°57′57″N; 10°56′46″E) is a remote high-alpine (2796 m a.s.l.) lake situated above treeline in the Ötztaler Alps (the Central Eastern Alps), Tyrol, Austria (Fig. 1). The maximum depth is 17.5 m and the surface area is 3.5 ha. About 1.5 ha of the lake bottom is covered with soft sediment. The lake has been monitored annually since 1985 by the Institute of Ecology, the University of Innsbruck. The lake is oligotrophic with a concentration of total phosphorus <5 μg l^{-1}. From 1985 to 2008, conductivity has increased from 10 to 31 μS cm^{-1}. At the same time the mean lake-water pH has increased from 5.6 to 6.1.

The basin lacks well-developed inflows and outflows. The catchment has an area of ca 18.0 ha with ca 1.2 ha mountain permafrost and rock glaciers (Thies et al., 2007). The underlying bedrock is mainly composed of granitic gneisses and micaschist with considerable amounts of arseno-pyrites (Koinig et al., 1998). The soil cover of the catchment area is thin and a large proportion of the catchment consists of bare rocks. Currently, the ice cover typically lasts for about nine months per year (November–July) which results in the onset of anoxic conditions in sediments and bottom-water layers of the deepest zone.

Snow accounts for 75% of the annual precipitation and during cold periods the slopes in the catchment area are covered by snow (Sommaruga-Wögrath et al., 1997). However, perennial snow fields around the lake have disappeared since the 1980s, and after ca 1990 wet precipitation (rain) exceeds the dry precipitation (snow) (Efthymiadis et al., 2006; R. Böhm, pers. communication). The modern mean January and July air temperatures based on meteorological measurements in the region for the period of 1977–2006 and calculated for the altitude of SOS (temperature lapse rate of 0.65 °C per 100 m) are −9.6 °C and 4.1 °C, respectively (Böhm et al., 2001; R. Böhm, pers. communication).

3. Materials and methods

3.1. Field and laboratory methods

3.1.1. Coring, subsampling and chemical analyses

A 159 cm long sediment core (SOS05-P1) was obtained using a Piston corer 60 mm in diameter with a hydraulic core catcher function (UWITEC Corp., Austria) from a floating platform in the deepest part of SOS (17 m depth) during the ice free period in 2005. The core was sectioned contiguously into 1 cm thick samples in the laboratory and stored at 4 °C until further processing.

Sediment organic matter content for each sample was estimated as organic carbon (C_{org}) measured with Carlo Erba® elemental analyzer and calculated as a percentage of dry weight (DW). Total phosphorus (P_{tot}) was determined according to Vogler (1965). Several additional analyses (geochemical, mineralogical, mineral magnetic, pollen, and pigment) were carried out on the core that will be discussed by Koinig et al. (in preparation).

3.1.2. Sediment dating and age-depth modelling

The chronology of the sediment core was based on 9 accelerator mass spectrometry (AMS) radiocarbon dates derived from plant

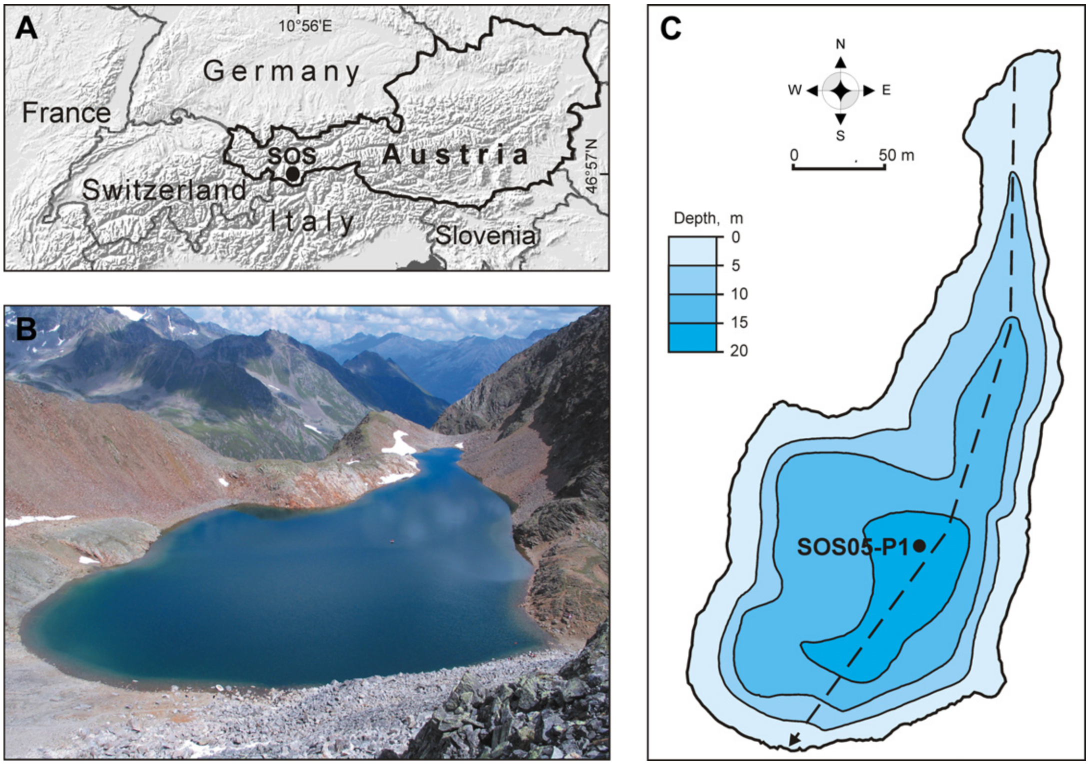

Fig. 1. (A) Map showing the location of Schwarzsee ob Sölden (SOS) in the Alpine region. (B) Photograph of SOS and its catchment, looking towards the north. (C) Bathymetric map of SOS showing the coring site (closed circle) and the modern zoobenthos sampling transect (dashed line).

macrofossils (Table 1), and on ^{210}Pb, ^{137}Cs, and ^{241}Am profiles for the top 8 cm of the core. The AMS radiocarbon dating was performed at the University of Vienna, Austria, and the ^{210}Pb, ^{137}Cs, and ^{241}Am dating at the University of Heidelberg, Germany. The radiocarbon ages were calibrated to calendar years Before Present (cal. BP), where 'present' is AD 1950, with the program OxCal v. 3.10 (Bronk, 2005), using the radiocarbon calibration curve IntCal04 (Reimer et al., 2004). All calendar-year ages were expressed with 95.4% probability envelopes. Age-depth relationship was established by means of a generalized mixed-effect regression and cubic spline interpolation (Fig. 2). The procedure uses mid-point estimates of the calibrated ages in combination with the central distributional range as the basis for estimating the fixed relationship between age and depth (Heegaard et al., 2005). According to this model, the samples from the core cover a time period of ca 10 200 years and the SOS record exhibits a mean depositional rate of 65 yr cm^{-1} (from 8 to 124 yr cm^{-1}). The top 1 cm layer of the sediment core was dated 1990 AD.

3.1.3. *Sampling of contemporary aquatic macroinvertebrates*

Contemporary chironomid larvae and other benthic macroinvertebrates were sampled on 28 July 2008, two weeks after the ice break. Fifteen macroinvertebrate samples were collected at 2.5–3.0-m depth intervals along a transect across the deepest point in the lake. The samples were taken with a standard kick net (mesh size of 100 μm, mouth 30 cm × 30 cm) in the upper littoral (0.5–1.5 m depth), and with an Ekman grab (10 cm × 10 cm) in the deeper zone. The samples were sieved (mesh size of 100 μm) in the field and hand-sorted under a stereomicroscope in the laboratory, where invertebrates were identified at 100–400× magnification to the species level when possible.

Table 1
Radiocarbon dates of samples from the SOS05-P1 sediment core.

Sample depth (cm)	Sample. no.[a]	Material dated	δ^{13}C (‰ VPDB)[b]	Reported age ($\pm 1\sigma$, ^{14}C yr BP)	Calibrated age (mid intercept, cal yr BP)	Calibrated age (2σ range, cal yr BP)
24–25	VERA-50056	Moss remains and unidentified twig/root	−70.7	2120 ± 60	2085	1860–2310
26–27	VERA-50093	Unidentified twig/root	−64.2	2155 ± 55	2160	2000–2320
34–35	VERA-50057	Moss remains and unidentified twig/root	−27.8	2470 ± 30	2575	2430–2720
60–61	VERA-50095	Moss remains	−45.8	3920 ± 40	4340	4230–4450
69–70	VERA-50096	Unidentified twig	−59.1	4600 ± 40	5370	5270–5470
83–84	VERA-50048	Unidentified twig/root	−24.4	5095 ± 30	5830	5740–5920
114–115	VERA-50097	Moss remains	−37.6	6785 ± 40	7630	7580–7680
127–128	VERA-50058	Bud scale	−27.9	7320 ± 30	8110	8030–8190
147–148	VERA-50059	Moss remains and unidentified twig/root	−21.1	8650 ± 30	9610	9540–9680

[a] VERA (Vienna Environmental Research Accelerator), University of Vienna, Austria.
[b] VPDB (Vienna Pee-Dee Belemnite).

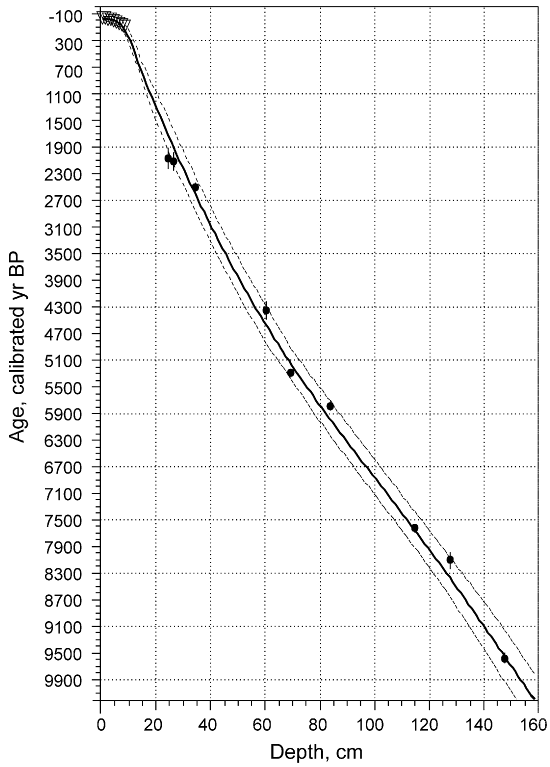

Fig. 2. Depth-age model for the SOS sediment profile (continuous line); dashed lines indicate upper and lower 2σ ranges for depth–age relationship. The median probability of calibrated ^{14}C dates is shown by closed circles and the upper and lower bounding date (±2σ) by vertical lines. ^{210}Pb dates are plotted as empty triangles.

3.1.4. Fossil chironomid analysis

All 159 sediment samples from the core SOS05-P1 were analyzed for fossil chironomids. Chironomid remains were extracted from the fresh sediment without chemical treatment, following Walker (2001). Wet sediment (0.3–15.5 g) mixed with distilled water was sorted in a Bogorov counting tray under a dissecting microscope at 25–40× magnification. Chironomid remains were picked out, dehydrated in 100% ethanol and slide-mounted ventral side up in Euparal® for taxonomic identification. Given that a minimum of 50 head capsules (HC) per sample provides a representative count for reliable temperature reconstructions (Heiri and Lotter, 2001), at least 50 chironomid head capsules were counted and identified in each sample (mean = 58 HC); five samples (0.5 cm, 27.5 cm, 50.5 cm, 130.5 cm and 144.5 cm) contained only 38–45 head capsules. Chironomid concentration was calculated as head capsule abundance per gram dry sediment (HC g^{-1} DW). Chironomid accumulation rate in the sediment was calculated as influx of head capsules per square centimeter per year (HC cm^{-2} yr^{-1}).

Chironomids were identified at 100–400× magnification with a compound microscope and identification keys by Wiederholm (1983) and Brooks et al. (2007). The *Pseudodiamesa* head capsules were identified to specific level using the description in Ilyashuk et al. (2010).

3.2. Numerical methods

All stratigraphic diagrams were produced with the software TGView (Grimm, 2004) and the program C^2 v. 1.5 (Juggins, 2003). Prior to all numerical analyses, the chironomid percentage data were subjected to a square root transformation to stabilize variances among taxa.

3.2.1. Zonation

Chironomid zones were delimited with the technique of optimal splitting by information content (Birks and Gordon, 1985), and statistically significant zones were identified with the broken-stick approach (Bennett, 1996), using the software package Psimpoll 4.10 (Bennett, 2002). This approach yielding the highest variance reduction was taken to focus on long-term dynamics, as opposed to the highly variable shorter-term dynamics.

3.2.2. Multivariate analyses

A preliminary detrended correspondence analysis (DCA) of the chironomid data indicated a relatively short gradient along the first DCA axis (2.147 SD units), suggesting that linear ordination methods are appropriate for analyzing the data set. Principal components analysis (PCA), as indirect ordination technique based on Euclidean distances, was applied to the chironomid stratigraphy in order to interpret and summarize the major patterns of variation within the chironomid data. The statistical significance of the first two PCA axes was assessed by comparison with the broken-stick model (Legendre and Legendre, 1998). All ordinations were accomplished with the program CANOCO 4.5 and plots were created with CanoDraw 4.1 (ter Braak and Šmilauer, 2002).

3.2.3. Palaeotemperature inference model and reconstruction

A modern calibration data set from the Alpine region was used for the temperature reconstruction from the SOS chironomid record. The data set consists of subfossil chironomid assemblages in the surface sediments of 100 lakes at altitudes from 409 to 2815 m a.s.l. in the Swiss Alps, the Swiss Plateau, and the Jura Mountains (Heiri et al., 2003; Heiri and Lotter, 2005, 2008; Bigler et al., 2006) and describes the distribution of 96 chironomid taxa over a mean July air temperature (T_{July}) gradient of 5.0–18.4 °C. Since SOS is close to the lower limit of the temperature gradient in the Alpine chironomid-temperature calibration data set, we tried carefully to select the most reliable and appropriate model (i.e. the 'minimal adequate model' *sensu* Crawley, 1993) based on the available data set. According to Birks (1998) such a model should be as simple as possible and it should contain no redundant parameters or components. The leave-one-out cross-validation was used to evaluate the performance of developed transfer functions based on weighted averaging (WA; Birks, 1995) and weighted averaging-partial least squares regressions (WA-PLS; ter Braak and Juggins, 1993). A two-component WA-PLS model provided slightly better performance statistics than simpler WA method. However, comparison of the WA and WA-PLS chironomid-inferred T_{July} with an instrumental temperature record covering the time interval 1760–2005 for the study site revealed that most instrumental temperatures fall within the error bars of the WA inferred temperatures while the WA-PLS inferred temperatures were about three degree overestimated. Therefore, the WA model was applied to the chironomid record from SOS. This chironomid-temperature inference model based on WA with inverse deshrinking had a coefficient of determination (r^2) of 0.83, a root mean square error of prediction (RMSEP) of 1.56 °C, and a maximum bias of 1.52 °C as assessed by leave-one-out cross-validation. Sample-specific prediction errors (SSPEs) were estimated by Monte Carlo simulation (999 bootstrap cycles) following Birks et al. (1990). The reconstructed values were smoothed along time with a LOESS regression (Cleveland et al., 1993) and a span of 0.05 to highlight the main temperature trends during the Holocene. The reconstruction and all calculations were performed with the program C^2 1.5 (Juggins, 2003).

3.2.4. Reconstruction diagnostic statistics

The modern analogue technique with chi-square distance as the dissimilarity coefficient was used to identify the similarity between

each analyzed subfossil assemblage and the most similar subfossil assemblage within the modern calibration data sets (Birks et al., 1990). A cut level of the 2nd and 5th percentile of all chi-square distances within the modern data was taken to identify samples with no 'close' and no 'good' closest analogue in the modern calibration data, respectively.

Goodness-of-fit statistics derived from a canonical correspondence analysis (CCA) of the modern calibration data and down-core passive samples with T_{July} as the sole constraining variable was used to assess the fit of the analyzed down-core assemblages to temperature (Birks et al., 1990; Birks, 1995, 1998). This method allows an assessment of how unusual are the fossil assemblages in respect to the composition of the training set samples along the temperature gradient. Fossil samples with a residual distance to the first CCA axis larger than the 90th and 95th percentile of the residual distances of all the modern samples were identified as samples with a 'poor fit' and a 'very poor fit' with T_{July}, respectively (Birks et al., 1990). Furthermore, chironomid taxa in the down-core record with a Hill's N2 (Hill, 1973) below 5 in the calibration data were considered to be rare in the modern data set (Heiri et al., 2003, 2007a). Chi-square distance and Hill's N2 values were calculated with the program C^2 1.5 (Juggins, 2003), and CCA was accomplished with the program CANOCO 4.5 (ter Braak and Šmilauer, 2002).

4. Results and interpretation

4.1. Contemporary communities

The depth transect is characterized by varying substrate from slightly silted stones at 0.5–3.0 m depth to light silt at intermediate depths and to black silt at the deepest area (16.5–17.5 m) of the lake (Figs. 1 and 3). In addition, submerged macrophytes represented by the aquatic moss *Sphagnum* form a dense mat as a narrow band at the lower sublittoral (ca 9–10 m depth) in the northern part of the lake. The moss phytomass is ca 150–200 g air-dry weight m^{-2}. In temperate regions, aquatic mosses forming the dominant submerged vegetation in transparent softwater lakes are known from the Austrian Alps (Pechlaner et al., 1972) and other mountain areas (e.g., Light, 1975) as well as from northern lowland areas (Toivonen and Huttunen, 1995; Ilyashuk, 2002), where they colonize great depths although the lakes are ice-covered up to 8–10 months a year.

Analyses of the invertebrate samples showed that the benthic invertebrates are represented by chironomid larvae (3 taxa) and oligochaete worms (Annelida: Oligochaeta; 3 taxa). Only single chironomid larvae of *Micropsectra radialis* were found at the black silt of the deepest part of the lake, while the oligochaete *Tubifex tubifex*, able to survive hypoxia (Volpers and Neumann, 2005), dominates the invertebrate communities, reflecting unfavorable oxygen conditions in sediment within this small part of the lake bottom.

The distribution of the chironomid *Corynoneura arctica* in the lake indicates that it dwells in the upper littoral (0.5–1.5 m depth) with slightly silted stones, where its relative abundance reaches 100%, and inhabits also *Sphagnum* mats of the lower sublittoral (9–10 m depth), reaching an abundance of 20%. Apparently, C. *arctica* prefers periphyton habitats and is an important component of epilithic communities within the stony littoral and epiphytic communities within the submerged bryophytes of the sublittoral. This species is widespread in the Alps where it prefers periphyton habitats of slightly acid lakes (Boggero et al., 2006). It should be mentioned that the *Corynoneura* remains were not recorded in the surface sediment sample of the studied core retrieved from the deepest part of the lake. Therefore, transport of chironomid remains from shallower areas to the deepest part of the lake does not seem to be a very active taphonomic process within SOS.

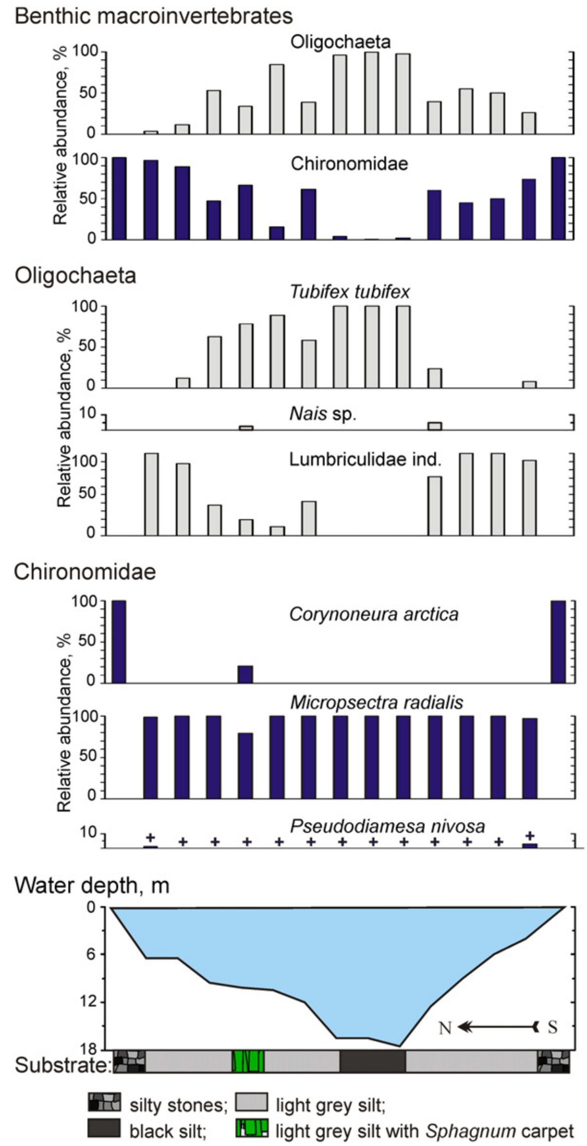

Fig. 3. Structure and distribution of contemporary benthic macroinvertebrate communities and oligochaete and chironomid assemblages along the depth transect in SOS on 28 July 2008 (two weeks after the ice break). Plus sign denotes the presence of head capsules on the surface of sediment (see text for details).

The chironomid *M. radialis*, the most abundant chironomid species in the lake (80–100%), occurs across a wide bathymetric range among soft detritus sediment, except in the upper stony littoral. Only one larva (at 6.5 m depth) and one pupa (at 4 m depth) of *Pseudodiamesa nivosa* was found in the zoobenthos samples, whereas a great number of head capsules of this taxon was observed on the surface of soft sediment in the samples from 4.0 to 17.5 m depth. Apparently, mass emergence of *P. nivosa* started simultaneously with the beginning of ice cover break-up, when the first cracks appear in the ice cover through which the *Pseudodiamesa* adults are able to emerge successfully (Oliver, 1968), and finished shortly after a complete disappearance of ice cover in mid July.

M. radialis and *P. nivosa* often dominate together in lakes at altitudes above 2000 m (Rieradevall et al., 1999; Tátosová and Stuchlík, 2006). Both taxa are cold-adapted. However, it is known that the genus *Pseudodiamesa* is more adapted to harsh physical environments, including freezing and drying. For example, *P. nivosa*

dominates usually in glacier-fed streams, and its distribution is explained by temperature through 105 sites from Svalbard to the French Pyrenees (Lods-Crozet et al., 2001). The larvae of *Pseudodiamesa* are able to complete their life cycle even if water temperatures never exceed 2 °C (Milner et al., 2001). The adults of *Pseudodiamesa* can emerge successfully through cracks in the ice cover at the beginning of thawing (Oliver, 1968; Danks and Oliver, 1972), and copulate on the snow cover at subzero (−1 to −2 °C) air temperatures (Hågvar and Østbye, 1973). *M. radialis*-type, a common colonizer of northern and alpine lakes, has a more widespread distribution in respect to temperature than *Pseudodiamesa* according to several lake training sets (Larocque et al., 2001; Bigler et al., 2006; Heiri and Lotter, 2008) and, most likely, is less cold-adapted than *P. nivosa*-type.

4.2. Subfossil chironomid assemblages

4.2.1. Down-core record

Chironomid concentrations varied from 13 to 1164 HC g^{-1} of dry sediment throughout the core. Twelve chironomid taxa were identified in the sediment sequence, eight thereof have abundances >2% in at least two samples. Rare taxa (abundance <2%) are *Psectrocladius sordidellus*-type, *Diamesa*, *Paraphaenocladius*, and *Heterotrissocladius marcidus*-type. The photographs of the most abundant taxa are presented in Fig. 4.

The down-core changes in the chironomid record are pronounced. Seven statistically significant zones were determined in the chironomid stratigraphy (Fig. 5). The following qualitative inferences are based on available knowledge about ecological preferences of the dominant taxa.

Zone Ch-1 (159–155 cm; ca 10 200–10 000 cal yr BP) is dominated by cold-adapted *P. nivosa*-type and *M. radialis*-type. The chironomid concentration is low. This zone represents the pioneer stage of the aquatic ecosystem when chironomid species began to colonize the lake forming after deglaciation. Apparently, a rapid climatic improvement after the Younger Dryas stadial caused the melting of perennial ice and the topographic depression filled with cold meltwater that formed this lake. It is likely that dead-ice has remained in the lake and/or in the catchment during this period. These conditions would have been particularly favorable for

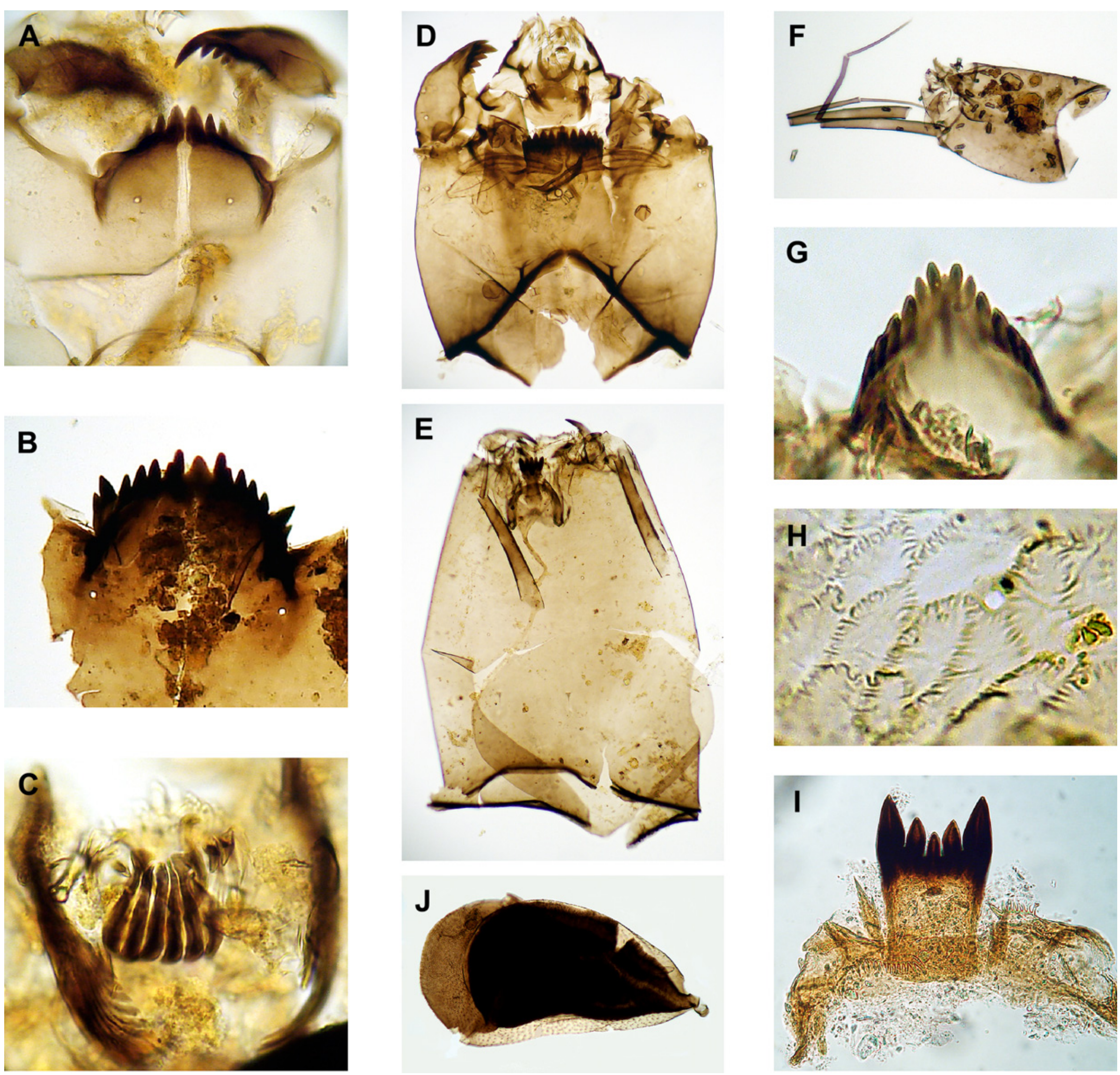

Fig. 4. Photos of subfossil chironomid remains from SOS: A – *Heterotrissocladius grimshawi*-type; B, C – *Pseudodiamesa nivosa*-type; D – *Micropsectra radialis*-type; E – *Zavrelimyia* type A; F, G, H – *Corynoneura arctica*-type; I, J – *Procladius* (*Holotanypus*). A – mentum and mandibles; B, G – mentum; C – premandibles and pecten epipharyngis; D, E, F – head capsule, ventral view; H – strong net-like reticulation on head capsule; I – ligula and paraligulae; J – thoracic horn of pupa.

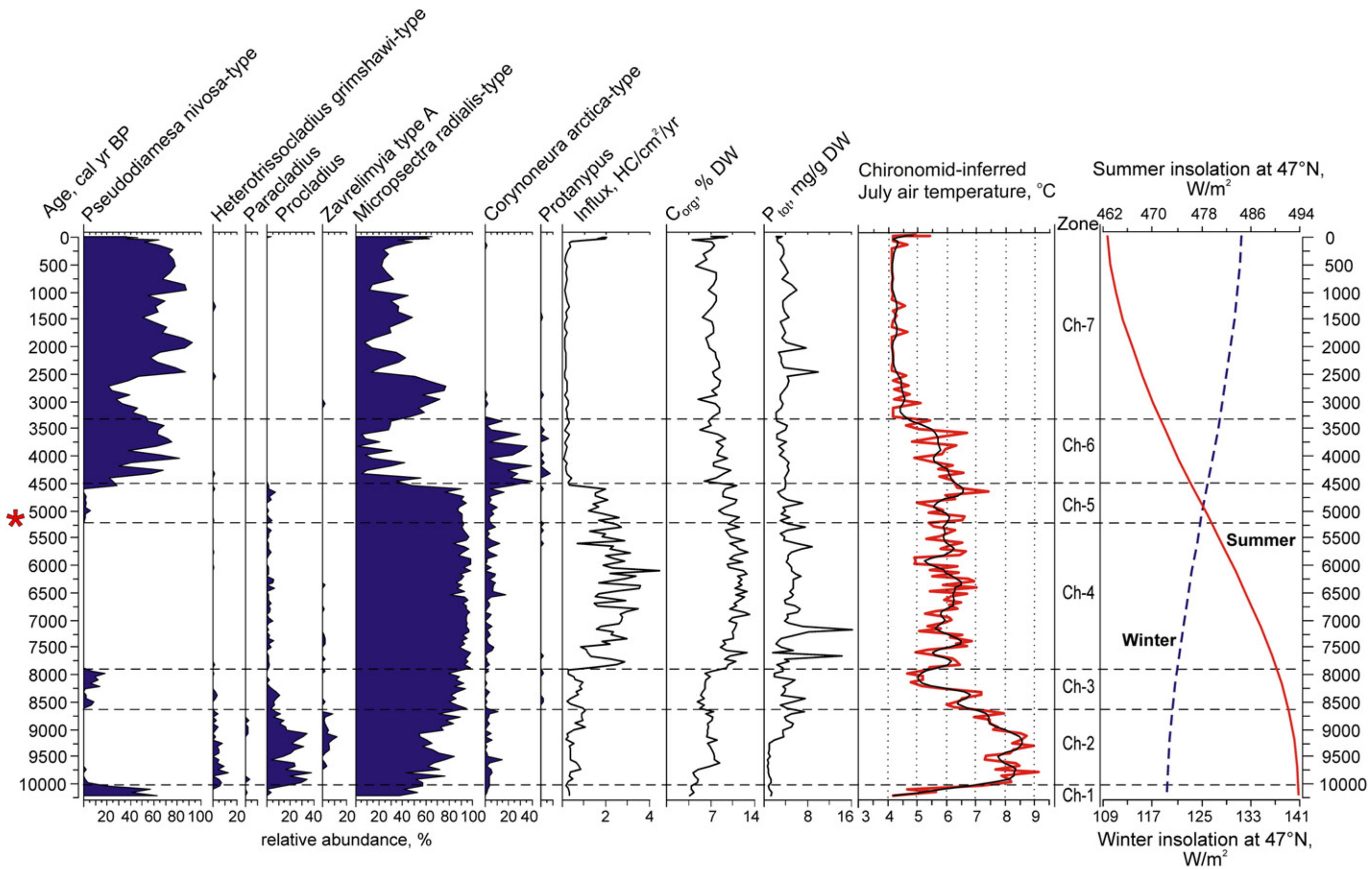

Fig. 5. Percentage abundance of selected chironomid taxa in the SOS record, total accumulation rate of chironomid head capsules (Influx, HC cm^{-2} yr^{-1}), sediment organic content expressed as percentage of organic carbon (C_{org}, % DW), total phosphorus concentration in sediments (P_{tot}, mg g^{-1} DW), the chironomid-inferred mean July air temperature (T_{July}, °C; thick line represents unsmoothed data, and thin line – a LOESS smoother with a span of 0.05), statistically significant zones for chironomid assemblages (dotted lines), and mean summer (June–August) and winter (December–February) insolation at 47°N (Laskar et al., 2004). The asterisk indicates the age of the Neolithic Iceman "Ötzi" (5300–5050 cal yr BP) found in the Ötztaler Alps at 3210 m a.s.l., ca 25 km from SOS (Bonani et al., 1994).

P. nivosa-type, adapted to survive in glacier-fed streams and cold-water lakes. Its presence in the bottom core layers likely reflects cold conditions resulting from input of cold meltwater under climate warming. Thus, the pioneer chironomid assemblages do not reflect the warm air temperature that caused the deglaciation but the cold aquatic environment resulting from meltwater input from the snow fields and glaciers still present in the catchment. Similar conditions were reconstructed in a lake in the Central Swiss Alp for the Lateglacial deglaciation (Ilyashuk et al., 2009).

Zone Ch-2 (155–132 cm; ca 10 000–8600 cal yr BP) is characterized by the disappearance of *P. nivosa*-type and a distinct increase in *M. radialis*-type. This shift is accompanied by an increase in the profundal taxa *Procladius* and *Heterotrissocladius grimshawi*-type (Bretschko, 1974; Tátosová and Stuchlík, 2006), as well as by the appearance of *Zavrelimyia* type A, a littoral dweller of high-alpine lakes (Brooks et al., 2007), and an increase in the periphyton inhabiting *C. arctica*-type. Sediment organic matter content and chironomid influx increased during this period. The presence of taxa commonly preferring warmer and shallow habitats implies an increase in productivity of the lake, especially of its shallow zone, which was apparently related to warm summers during this period. Concentration of total phosphorus (P_{tot}) of the sediments remained low during the first half of this period but increased rapidly thereafter, i.e. at ca 9200 cal yr BP. Despite high temperatures, productivity of the lake ecosystem must have been strongly limited by the low nutrient supply, especially before ca 9200 cal yr BP, as indicated by low P_{tot} values (Fig. 5). The high proportion (up to 43%) of facultative predators, i.e. *Procladius* and *Zavrelimyia* type A from the subfamily Tanypodinae, which are located at the top of the food web in benthic communities (Pinder, 1986), suggests rather complex species interactions in the lake ecosystem during this warm period.

Zone Ch-3 (132–119 cm; ca 8600–7900 cal yr BP) is distinguished by reappearance of *P. nivosa*-type and disappearance of the more warm-adapted *Zavrelimyia* type A. The change in the chironomid assemblages may be related to a cooling during this period. The lower organic carbon (C_{org}) and total phosphorus (P_{tot}) values of the sediments suggest a decrease in lake productivity.

Zone Ch-4 (119–70 cm; ca 7900–5200 cal yr BP) displays an absolute dominance of *M. radialis*-type and an absence of *P. nivosa*-type. This suggests that warmer climate prevailed during this long time period. The highest chironomid influx in the zone may indicate an increased overall productivity in the lake (Alm and Willassen, 1993), what is also reflected by high sediment organic matter content.

Zone Ch-5 (70–59 cm; ca 5200–4500 cal yr BP) is marked by reappearance of *P. nivosa*-type in abundances of 2–6% throughout most of the time. At the end of this period, its relative abundance reached 28%. Influx of chironomid remains, C_{org}, and P_{tot} show a tendency to decrease. All these changes suggest a gradual cooling and a decrease in lake productivity during this period.

Zone Ch-6 (59–43 cm; ca 4500–3300 cal yr BP) reveals a sudden change in the chironomid assemblages. *P. nivosa*-type began again to dominate in the lake, whereas abundance of *M. radialis*-type decreased. *C. arctica*-type became more common,

often reaching abundances of 15–40%, and chironomid accumulation rates decreased abruptly by about one order of magnitude. These major changes in the chironomid assemblages suggest rapid cooling while lower C_{org} and P_{tot} values through this zone indicate decreased lake productivity. Taking into account the habitat preferences of extant chironomids in SOS, the shift from *M. radialis*-type to *C. arctica*-type may be related to an extensive development of the aquatic mosses at the bottom of the lake preferred by *C. arctica*-type as habitat. An increase in water transparency, as a response to decreased nutrient levels and plankton community production during cooling, may have induced an increase in the depth limit of the mosses and their extension to the deeper part of the lake. A previous study at SOS (Koinig et al., 1998) has shown that temperature change is the main driving force for pH shifts in the lake. The supposed slow pH decline concomitant with the cooling should be favorable for the expansion of acid-tolerant submerged *Sphagnum* mosses (Raven, 1988) and the associated chironomid *C. arctica*-type which prefers slightly acid lakes (Boggero et al., 2006).

Zone Ch-7 (43–0 cm; ca 3300–0 cal yr BP) is defined by the predominance of only two chironomid taxa, *P. nivosa*-type and *M. radialis*-type. Chironomid total accumulation rate remained low almost during the whole period, except for the past century. Altogether, this period was cold, but rather unstable. Apparently, further climate deterioration apparently has led to cooler winters, a longer duration of ice cover, and a decrease in light availability. Thus, favorable conditions for mosses may have declined markedly and *C. arctica*-type has disappeared from the record by the end of this period, although as described above it is still present in the shallow littoral part of the lake today. Abrupt changes in the relative abundance *P. nivosa*-type and *M. radialis*-type indicate that temperature oscillations of different magnitude and duration occurred during the rest of the Holocene. For instance, the lowest abundance of *P. nivosa*-type (21–47%) occurred at ca 3200–2500 cal yr BP and since the beginning of 20th century, suggesting that these periods were warmer than when abundance of this cold-stenothermic taxon was higher (50–93%).

4.2.2. Down-core ordination

The PCA ordination applied to the chironomid stratigraphy from SOS provides a clear overview of environment preferences of the taxa in the lake, which is quite extreme due to its high-altitude location. The first PCA axis accounts for 73.2% of cumulative variation in the chironomid data, and the second for 11.5%. According to comparisons with the broken-stick model, only the first axis accounts for a significant amount of the variation. The PCA ordination (Fig. 6) reveals that the scores of the key species, *P. nivosa*-type and *M. radialis*-type, occupy opposite extremes along the first PCA axis; *P. nivosa*-type has the highest positive score on this axis while *M. radialis*-type shows the lowest negative score. Changes in the first axis scores clearly separate the assemblages dominated by cold-stenothermic *P. nivosa*-type (Zones Ch-1, Ch-6 and Ch-7), from all other assemblages (Fig. 6). Taking into account the species scores and the distribution of the chironomid assemblages, the first PCA axis is interpreted to mainly reflect a temperature gradient. Although both taxa are regarded as cold-adapted, *P. nivosa*-type and *M. radialis*-type reveal the opposite preferences along the first PCA axis. However, from several existing lake training sets (Larocque et al., 2001; Bigler et al., 2006; Heiri and Lotter, 2008) it is well established that *M. radialis*-type has a more widespread distribution in respect to temperature than the cold-stenothermic *P. nivosa*-type, which even manages to copulate on the ice cover (Hågvar and Østbye, 1973). Consequently, these two taxa are separated in a remote high-altitude site like SOS where cold temperatures are the norm and cold-adapted species compete along highly and less severe cold temperatures.

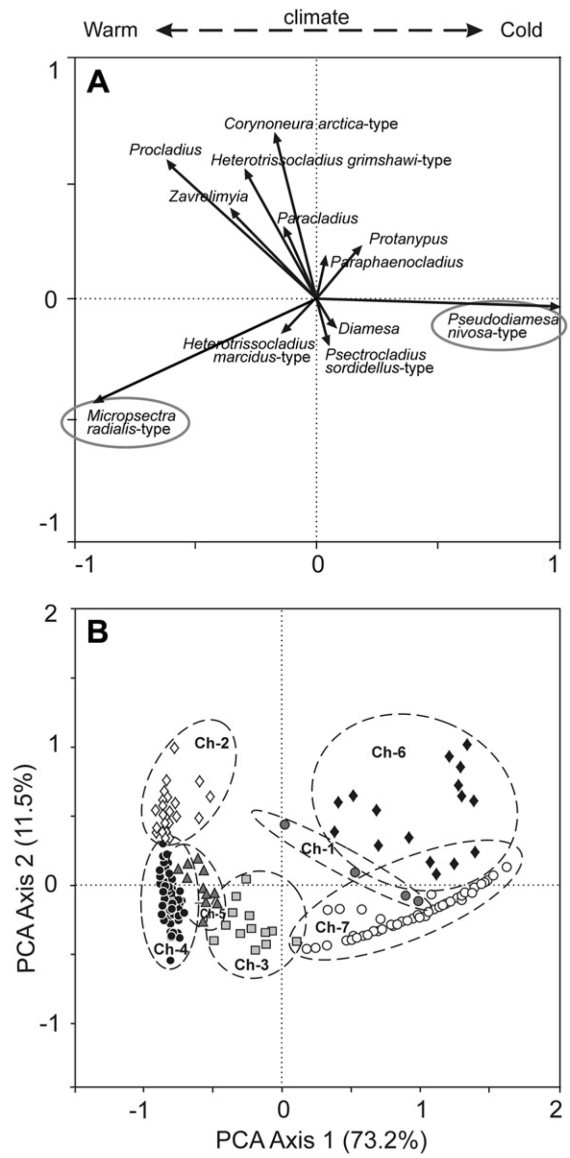

Fig. 6. Scatter plots of a principal components analysis (PCA) of the SOS chironomid stratigraphy (SOS05-P1) showing the species scores (A) and the sample scores (B).

In respect of the second PCA axis, *C. arctica*-type associated with periphyton habitats on the surface of stones and submerged mosses in the lake, the facultative predators *Procladius* and *Zavrelimyia*, and the profundal inhabitant *H. grimshawi*-type indicative of oligotrophic well-oxygenated conditions are characterized by the highest positive score, while *M. radialis*-type dwelling in soft sediment has the lowest negative score. This suggests that changes in the chironomid assemblages along the second PCA axis are driven by different factors, which may be associated with climate changes. This axis may integrate environmental driving forces such as changes in substrate type, trophic conditions, oxygen availability, and other possible factors influencing the composition of the chironomid assemblages in the lake. The distribution pattern of the chironomid assemblages along the second PCA axis reveals that the assemblages of the transitional periods (Zones Ch-2 and Ch-6) are located in the upper part of the ordination and consist of taxa which likely profit from the shift in dominant species caused by a rapid change in environmental conditions, whereas the assemblages formed at relatively stable environment and characterized

by lower species richness are located in the lower part of the ordination. Noticeably, *P. nivosa*-type tends to score near zero on the second PCA axis, suggesting that factors other than temperature played a minor role in its distribution in the lake through time.

4.3. Quantitative temperature reconstruction

4.3.1. Reconstruction diagnostic statistics

All subfossil taxa found in the SOS down-core samples are well represented in the training set used to develop the applied chironomid-temperature transfer function and no taxon in the fossil record has been identified as rare in the modern data. All samples have a 'close' analogue in the modern calibration data set (Fig. 7). Goodness-of-fit statistics revealed, however, that only 3 samples have a 'good' fit, 19% of the samples have a 'poor' fit and 79% have a 'very poor' fit with temperature. These lack-of-fit measures indicate that most fossil chironomid assemblages have no strong modern analogues in terms of similar relative chironomid abundances in the modern calibration set. Hence temperature reconstructions from the SOS record may be rather problematic, especially through the late-Holocene, which includes the samples with particularly high residual distance to the first CCA axis with T_{July} as the sole constraining variable, and individual temperature estimates should be considered as tentative and interpreted with caution. However, CCA goodness-of-fit measure does not *sensu stricto* evaluate whether inferred values accurately reflect past conditions and may not always give correct information on a reliability. 'Poor' fit samples may provide accurate estimates while 'good' fit samples may not always provide correct results (Bigler et al., 2002; Velle et al., 2005).

We suppose that a smoothing technique, namely a LOESS smoother, used usually to reduce random fluctuations in a data series will provide a clearer view of the true underlying behavior of the data and help to highlight temporal trends. Therefore our interpretations focus mainly on the smoothed values, rather than on inferences from individual data points.

4.3.2. Holocene July air temperature

The inference model provided the chironomid-based T_{July} profile shown in Fig. 5. The smoothed reconstruction indicates that T_{July} was between ca 4.0 and 8.5 °C over the Holocene. In Zone Ch-1 (10 200–10 000 cal yr BP), the inferred T_{July} rose rapidly from ca 4–7 °C. For the samples of Zone Ch-2 (10 000–8600 cal yr BP), the model reconstructs the highest temperatures (ca 7.0–8.5 °C) of the entire record, i.e. 3.0–4.5 °C above the modern value (mean T_{July} for 1977–2006). Later, through Zone Ch-3 (8600–7900 cal yr BP), the inferred T_{July} curve shows a decline to values of around 5 °C by the end of the period. Within Zones Ch-4 and Ch-5 (7900–4500 cal yr BP), the temperature persists near 6 °C. Zone Ch-6 (4500–3300 cal yr BP) reveals a general decrease in T_{July} by ca 2 °C. Through much of Zone Ch-7 (3300 cal yr BP – present), T_{July} shows a nearly constant values of ca 4 °C, with an increase to ca 4.8 °C during the past century.

5. Discussion

5.1. Holocene climate variations

5.1.1. Early Holocene (ca 10 200–7900 cal yr BP)

The most notable feature of the Holocene climate at SOS is a well-defined early-Holocene thermal maximum (HTM) between

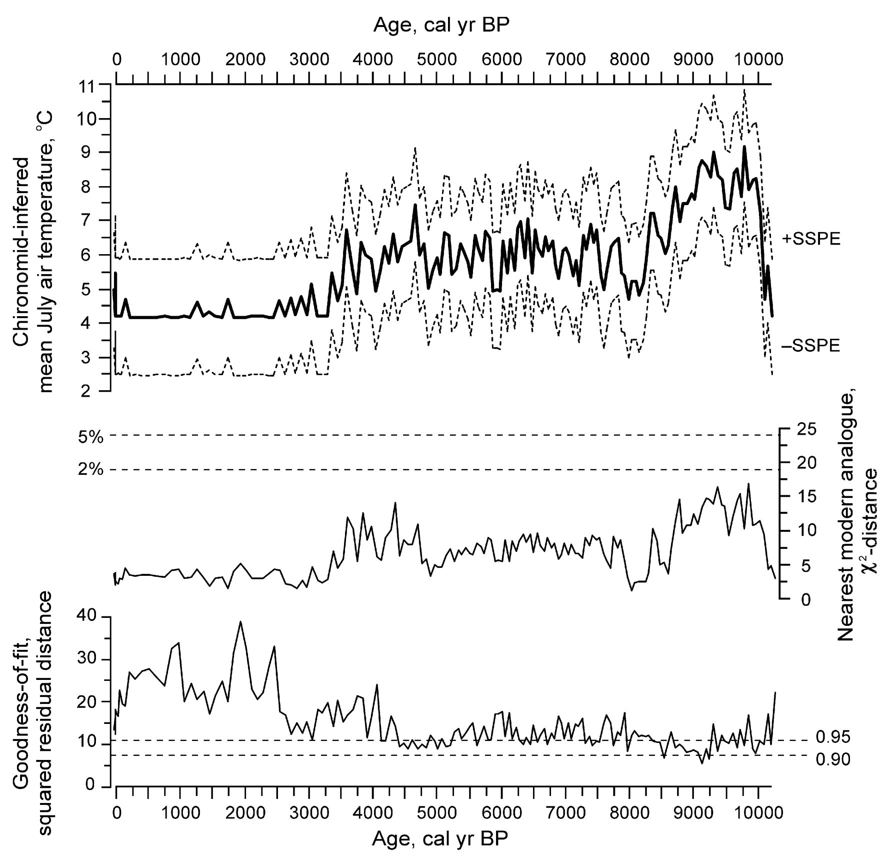

Fig. 7. Chironomid-inferred mean July air temperatures (solid line) from the SOS sediment core plotted together with sample-specific standard errors of prediction (SSPE, dashed lines), nearest modern analogues for the fossil samples in the calibration data set, and goodness-of-fit of the fossil samples with temperature. Horizontal dashed lines are used to identify samples with no 'close' (2%) and no 'good' (5%) modern analogues, and samples with 'poor' (0.90) and 'very poor' (0.95) fit with temperature.

ca 10 000 and 8600 cal yr BP, when chironomid-inferred T_{July} was 7.0–8.5 °C, i.e. up to ca 4.5 °C warmer than at present (mean value for 1977–2006). The timing of the warming is not consistent with recent climate model results and proxy records from the northern Swiss Alps, which have revealed that the timing of HTM in most parts of Europe falls approximately between 8 and 5 cal kyr BP (Renssen et al., 2009). Though the HTM at the middle and high latitudes of the Northern Hemisphere is generally associated with the orbitally forced summer insolation maximum, in much of the circum-Atlantic region, especially the mid latitudes, the HTM seems to have been delayed by the presence of the Laurentide ice sheet (LIS) in North America which has produced relatively cold surface-ocean conditions extending in an eastern direction towards western Europe (Renssen et al., 2009). There are a number of records form the Northern and Western Alps directly influenced by westerly winds which reveal similar temperatures through the early and middle Holocene or indicate a later HTM than the SOS record from the Eastern Alps (Heiri et al., 2003; Tinner and Theurillat, 2003; Heiri and Lotter, 2005; Larocque-Tobler et al., 2010). The Central Eastern Alps, however, are sheltered against westerly winds by mountain ranges of the Northern and Western Alps and characterized by a more continental climate. This may explain why temperatures in the Central Eastern Alps were less strongly affected by the early-Holocene cooling effect of the LIS and more strongly affected by changes in insolation than the more westerly part of the mountain chain. There is evidence that the maximum elevation of the forest limit (formed by *Pinus cembra* and *Larix*) in the Central and Southern Alps had already been reached during the early Holocene, suggesting that the warmest conditions since the beginning of the Holocene occurred ca 4000–5000 years earlier than in the Northern Alps (Lotter et al., 2006 and references therein). A chironomid record from the Central Swiss Alps (the Engadin valley, ca 110 km west of SOS) implies also that during most of the Preboreal T_{July} was above present-day values by ca 3 °C (Ilyashuk et al., 2009).

The magnitude of the early-Holocene warming at SOS, however, is not consistent with available treeline reconstructions in the Alps (Tinner and Ammann, 2001; Tinner and Theurillat, 2003; Nicolussi et al., 2005; Tinner, 2007), which reveal that the uppermost treeline position during the Holocene was about 180 m higher than today, indicating summer temperatures only about 0.8–1.2 °C higher than today. However, it should be noted that the treeline studies have been used for inferences of mean summer temperatures whereas our chironomid-based reconstruction refers to mean July temperatures, which are of course higher than average temperatures over summer. Furthermore, the early Holocene, characterized by the highest summer and the lowest winter solar radiation in the Northern Hemisphere (Kutzbach and Gallimore, 1988; Laskar et al., 2004) was a period of the greatest seasonal contrast with a prevalence of hot summers and cold winters (Fig. 5). In the northern mid-latitudes evaporation was at maximum and therefore moisture availability was minimal (Kutzbach and Webb, 1993). This is supported by the early-Holocene pollen-based climate inferences of Ortu et al. (2008) from the SW Alps which exhibit the highest T_{July}, while January and annual temperatures and annual precipitation were lowest. This period coincides with glacier retreats in the Austrian, Swiss, and Italian Alps indicative of dry conditions (Nicolussi and Patzelt, 2000; Hormes et al., 2006; Joerin et al., 2006). There is also evidence from a $\delta^{18}O$ stalagmite record in NW Italy (Grotta di Ernesto, 1165 m a.s.l.) that dry or dry-warm conditions prevailed during the early Holocene (9200–7800 cal yr BP) in the south-eastern Alps (McDermott et al., 1999). It is likely that these conditions may have impeded the expansion of tree species with high air and soil moisture requirements and extreme sensitivity to late frost in spring. A few studies (Lotter et al., 2006; Wehrli et al., 2007) have shown that these climatic conditions were favorable to thermophilic deciduous forests that prevailed in the Swiss Alps through the early Holocene.

Although SOS was always well above treeline, which never exceeded 2600 m a.s.l. even in the most favorable parts of the Alps (Tinner, 2007), pollen data from the SOS sediment record also reveal the highest concentration of long-distance transported pollen of *Corylus* and *Ulmus* (up to 20 and 10%, respectively) during this period (R. Drescher-Schneider, pers. communication), suggesting that thermophilic deciduous trees and shrubs were abundant at altitudes below 2800 m in the Ötztaler Alps only through the early Holocene. Similarly, quantitative pollen-based temperature inferences from three sites at altitudes 1920–2240 m a.s.l. in the Italian south-western Alps revealed the highest T_{July}, i.e. 2–5 °C higher than at present, in the early Holocene (Ortu et al., 2008) (Fig. 8).

The warmth peak was followed by a marked cooling that began after ca 9200 cal yr BP. This shift represents the most rapid cooling phase registered in the whole core. Between ca 8250 and ca 8000 cal yr BP, the inferred T_{July} dropped by about 3 °C compared to the HTM and indicated a T_{July} of ca 5 °C. This cold episode appears to be related to the abrupt climatic event about 8200 cal yr BP when a big outburst flood freshened the North Atlantic and widespread climatic anomalies developed across much of the Northern Hemisphere (Alley et al., 1997). A cooling period around 8200 cal yr BP has been detected also in other parts of the Austrian Alps based on sedimentological and biological proxies (Kofler et al., 2005; Schmidt et al., 2006). The pollen assemblages from two lakes in Switzerland and Germany also indicated a pronounced response of terrestrial vegetation to the climate change at ca 8200 cal yr BP (Tinner and Lotter, 2001). The climate shift to more humid and less continental conditions has been accompanied by glacier advances in the Eastern Alps (Nicolussi and Patzelt, 2001; Kerschner et al., 2006; Ivy-Ochs et al., 2009). A maximum relative cooling by ca 3 °C at 8200 cal yr BP was inferred from stalagmite $\delta^{18}O$ records from Katerloch Cave located in south-eastern Austria (Boch et al., 2009). Other reconstructions from Central Europe (von Grafenstein et al., 1998; Magny et al., 2001; Heiri et al., 2003; Magny and Bégeot, 2004) showed a temperature depression for the so-called '8.2-ka cold event' of 1.0–2.5 °C compared to the HTM, depending on the reconstruction method and location of the temperature record. According to temperature inferences based on $\delta^{15}N$ isotope records from the GISP2 ice core (Kobashi et al., 2007) and $\delta^{18}O$ records in the Agassiz and Renland ice cores (Vinther et al., 2009), temperatures in Greenland cooled by 3–4 °C during the 8.2-ka event.

5.1.2. Mid-Holocene (ca 7900–4500 cal yr BP)

During ca 7900–4500 cal yr BP, the average chironomid-inferred temperature was about 6 °C. It was a long stable and rather warm period and the lake productivity, as reflected by high sediment organic matter content and the highest chironomid accumulation rate, reached a maximum. As shown by pollen data, thermophilic deciduous forests in the Alps had been replaced by mesophilic silver fir-beech forests (Tinner and Lotter, 2001; Wehrli et al., 2007), suggesting lesser seasonal contrast and higher soil moisture availability. It is known that it was a period with high treeline position in the Alps (Tinner, 2007).

In spite of the fact that the smoothed chironomid-inferred temperature curve fluctuated near 6 °C during this period and did not reveal prominent changes before 4500 cal yr BP, a reappearance of *P. nivosa*-type around ca 5200 cal yr BP, after its absence of ca 2500 years in the chironomid record, suggests a cooling (Fig. 5) and concurs with a mid-Holocene climate reversal observed in the Alps. The finding of a mummified prehistoric man (the Neolithic Iceman 'Ötzi') dated to 5300–5050 cal yr BP in the Ötztaler Alps at 3210 m

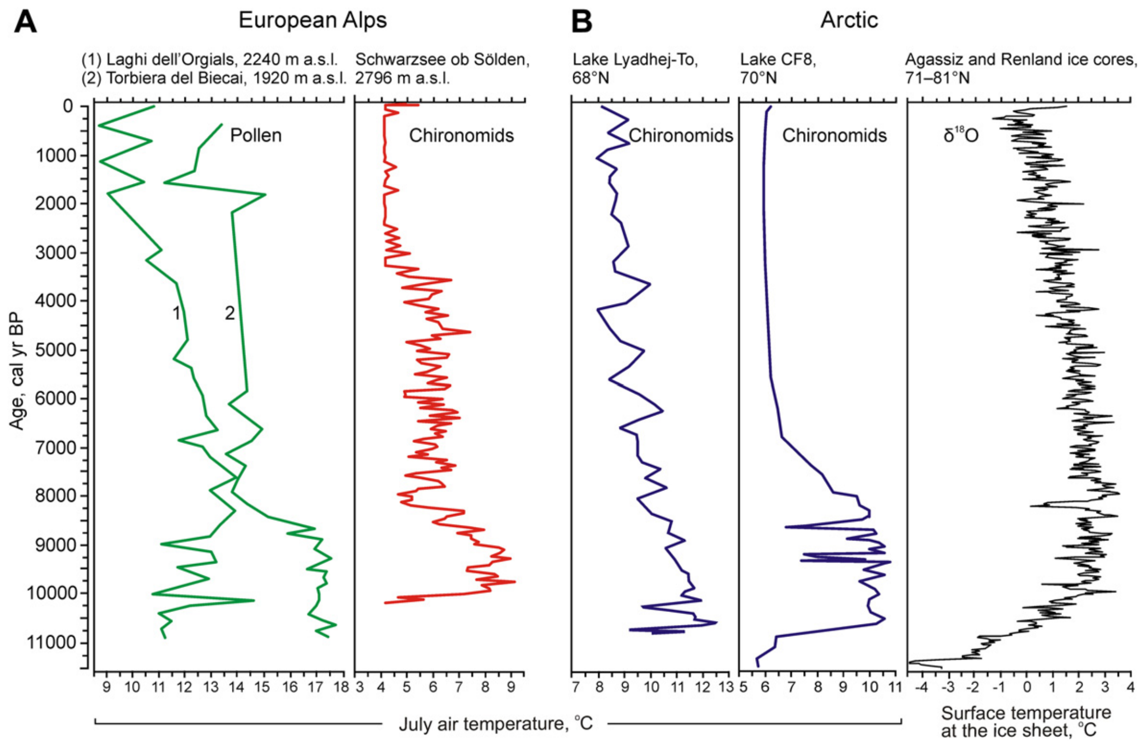

Fig. 8. Temperature inferences from: (A) high-alpine pollen records in the Italian Alps (Laghi dell'Orgials and Torbiera del Biecai; Ortu et al., 2008) and a chironomid record in the Austrian Alps (Schwarzsee ob Sölden; present study), and (B) high-latitude chironomid records in the Russian Arctic (Lake Lyadhej-To; Andreev et al., 2005) and the Canadian Arctic (Lake CF8; Axford et al., 2009b), and the Greenland ice-core $\delta^{18}O$ records (the Agassiz and Renland ice cores; Vinther et al., 2009).

a.s.l. (Bonani et al., 1994), ca 25 km from SOS, suggests that this cooling was accompanied by a rapid glacier expansion, which was responsible for the quick burial and preservation of the corpse by permanent snow cover on a previously deglaciated area (Baroni and Orombelli, 1996). A mid-Holocene climate reversal has been also observed in various regions of the world (Magny et al., 2006). There is strong evidence that the African Humid Period came to an end around 5500 cal yr BP, and climate became very dry in North Africa, responding to declining insolation and weakness of monsoon winds (Foley et al., 2003; Kröpelin et al., 2008). These events correspond to the Hypsithermal–Neoglaciation transition that may have been caused by variations in solar activity superimposed on variations in ocean and air circulation and suggest inter-hemispheric linkages for climate variations (Magny and Haas, 2004). Thus, a mid-Holocene climate shift which may be related to other climatic changes of global significance is clearly evident in the chironomid record from SOS (Zone Ch-5).

5.1.3. *Late Holocene (ca 4500–0 cal yr BP)*

The SOS chironomid record suggests that a sudden climatic change has occurred ca 4500 cal yr BP. Our reconstruction reveals low productivity of the lake and a general decrease in T_{July} until 2500 cal yr BP by about 2 °C. Similarly, the chironomid-based reconstructions from the Swiss Alps indicate a decrease in T_{July} around 4000 cal yr BP (Heiri et al., 2003; Heiri and Lotter, 2005) that was probably coupled to changes in summer and winter insolation (Fig. 5). The global climate system experienced a drastic reorganization during that time period. Megadroughts near 4200 cal yr BP were recorded at multiple mid-latitude and subtropical sites of the Northern Hemisphere: in North America, Europe, Africa, and Asia (Booth et al., 2005). Other proxy data from the Alps reveal glacier advances and timberline depressions after ca 4500 cal yr BP related to the development of cooler, wetter and more oceanic climate conditions in the region (Leeman and Niessen, 1994; Haas et al., 1998; Tinner and Theurillat, 2003).

The inferred T_{July} is on average ca 4.5 °C for ca 3200–2500 cal yr BP. In the Alps, this interval was characterized by rather frequent changes from cooler and more humid to warmer and drier conditions, and vice versa, prolonged glacier advances became more frequent and periods of recession were shorter (Ivy-Ochs et al., 2009). In the subsequent period, since ca 2500 cal yr, the reconstructed T_{July} shows nearly constant values of ca 4 °C. The recent decades are marked by an increase in T_{July} to ca 4.8 °C. The increasing influx of chironomid remains since the last decades may also reflect an increase in lake productivity in response to warmer summers, as interpreted elsewhere (e.g., Alm and Willassen, 1993).

5.2. *The early-Holocene thermal maximum: SOS versus other 'early-warning sites'*

Due to various positive-feedback mechanisms, climate changes are amplified in polar (high-latitude) and alpine (high-altitude) regions (ACIA, 2004; Parker et al., 2008). From a perspective of climate change research, polar and alpine regions are often considered to be so-called 'early-warning sites' (Ørbæk et al., 2004). Simulations of temperature changes along the axis of the American Cordillera, from Alaska to southern Chile, show that statistically significant amplitudes of summer temperature changes with elevation are especially large at latitudes between ca 35°N and 50°N, and suggest that mountain ranges that extend high into the lower troposphere here are likely to experience significant temperature alterations (Bradley et al., 2004). In the European Alps instrumental measurements indicated a total irradiance increase with altitude of ca 8% per 1000 m (Blumthaler et al., 1997) and it has been shown that temperature anomalies and trends stand out more clearly at higher elevation sites than in the adjacent lowlands

(Beniston, 2005). It should be noted that the location of SOS (ca 47°N) is within the latitudinal range, for which the largest summer temperature changes with elevation are modeled by Bradley et al. (2004).

Global radiation measurements carried out with identical instrumentation at a high-altitude station in the Swiss Alps (46°N; 3576 m a.s.l.) and at a high-latitude station in Alaska (64°N; 133 m a.s.l.) show that the global radiation maxima in summer are similar for the two sites (Ambach et al., 1991). Thus, polar regions and high-altitude sites in the Alps with similar present-day air summer temperatures may be characterized by a similar sun's output in summer and, most likely, insolation changes responsible for the HTM affected the polar and alpine regions with a similar strength, although in a different way, and therefore the HTM would have been similar in the timing and magnitude in these regions.

Chironomid-inferred temperatures from SOS indicate a comparable temperature development as the Holocene records from sites in the Arctic where the HTM was forced primarily by insolation changes and the effect of the Laurentide ice sheet on climatic conditions was not significant. Recent chironomid-based T_{July} reconstructions from lakes of Baffin Island, northeast Canada (70°N), revealed a similar pronounced HTM between ca 10 000 and 8500–8000 cal yr BP with T_{July} ca 5 °C warmer than today, in line with solar forcing (Briner et al., 2006; Axford et al., 2009a, 2009b). The latest inferences of the Holocene temperature history in Greenland (71–81°N) derived from the $\delta^{18}O$ records in the Agassiz and Renland ice cores placed the HTM there between ca 10 000 and 7000 cal yr BP (Vinther et al., 2009). Chironomid-based records from northern Iceland (65°N) suggest that temperatures were up to 2–2.5 °C warmer than present from ca 10 500–8500 cal yr BP (Langdon et al., 2010). Temperature reconstructions from the Russian Arctic also suggest a pronounced early-Holocene thermal maximum (Velichko et al., 1997; MacDonald et al., 2000; Andreev et al., 2005). For example, the temperature inferences based on pollen and chironomid records from a site in the Polar Urals (68°N) showed the HTM at ca 10 500–8800 cal yr BP with T_{July} ca 3–4 °C warmer than today (Andreev et al., 2005). While the individual records may have been somewhat varied when comparing northern and high-altitude European sites, maximum early-Holocene summer warmth reconstructed from chironomids and other proxies seems to have been of a comparable magnitude for the high-altitude Alps and Arctic regions (Fig. 8). Thus, the chironomid-based temperature record from SOS corroborates other studies revealing that the Holocene climate, particularly of polar and alpine regions, is very sensitive to insolation forcing.

5.3. Reliability of the inferred Holocene temperatures

The reliability of inferences is a key question in any quantitative proxy-based climate reconstruction. The temperature reconstruction presented here was carried out for a remote lake that is quite extreme due to its high-altitude location. It is known that mountain lake ecosystems are sensitive indicators ('sentinels') of environmental changes as a result of their hydrochemical characteristics, their relatively low diversity and their simple food webs (Adrian et al., 2009). With increasing altitude, climate-related ecological factors become dominant and, therefore, the effects of climate change may be more pronounced compared to ecosystems of lower altitude. On the other hand, it has been shown that alpine lakes in the European Alps, unlike lowland lakes, have a thermal regime in which their lake-water temperature in summer is indirectly linked to altitude, and the relationship of lake-water temperature to ambient air temperature weakens considerably on crossing a threshold altitude of 2000 m (Livingstone et al., 2005). In the case of chironomids, both lake-water and ambient air temperatures are physiologically important in governing their life cycles and distribution (Oliver, 1971; Armitage, 1995). The primary climate effect on the aquatic stages of chironomids (egg, larva, and pupa) in high-altitude lakes may be mediated also by the timing of the ice cover period (Livingstone et al., 1999), which may thus play a role in SOS. Chironomid-based inferences from SOS in terms of the air temperature may therefore have been affected by the indirect relation between air and water temperature in high-elevation lakes. We believe that an extension of the available data set from the Alpine region by lakes from higher altitudes, the development of a transfer function for summer water temperature and application to the chironomid record from SOS and other remote high-mountain lakes could provide more reliable Holocene summer temperature inferences from these sites unaffected by direct human impact.

Our temperature reconstruction, however, contains common imprints of climatic events in the region. Furthermore, the most powerful means of model validation (of how reliable are the results) is to compare the reconstructions against known instrumental environmental records (e.g., Birks, 1998; Velle et al., 2010). Comparison of the chironomid-inferred T_{July} with an instrumental meteorological record covering the time interval 1760–2005 reveals that most instrumental temperatures fall within the error bars of the inferred temperatures (mean ± SSPE) and 80% of the inferences for this period had deviations from the instrumental data below the RMSEP (Fig. 9). This suggests that long-term Holocene temperature trends may be quite reliably reflected in the temperature reconstruction. However, based on Fig. 9, the inferred temperatures seem to be about one degree overestimated during this period and, therefore, unsmoothed reconstructed temperatures should be interpreted with caution.

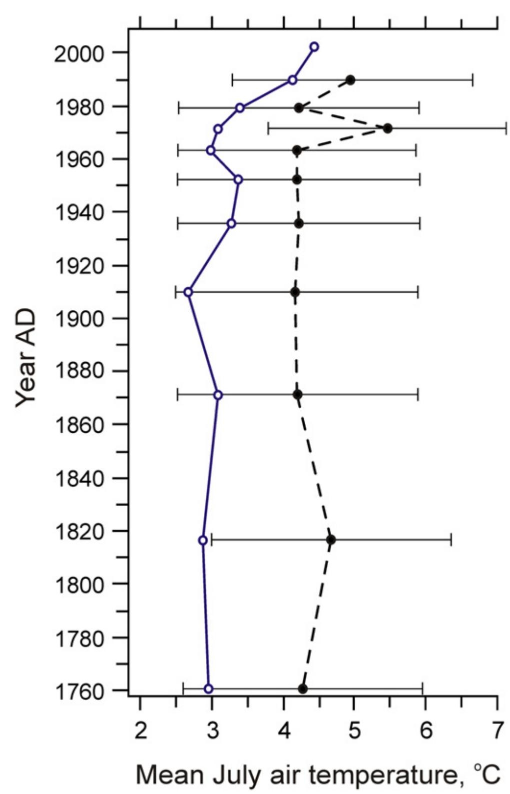

Fig. 9. Chironomid-inferred mean July air temperatures (solid circles) with the estimated errors as horizontal error bars (SSPE) from the SOS record plotted versus the meteorological data (open circles) at the region corrected for the altitude of SOS using a lapse rate of 0.65 °C per 100 m (R. Böhm, pers. communication). The meteorological data were modified by calculating mean temperatures for the time span covered by each chironomid sample.

One of potential problems within quantitative temperature reconstructions is that biota responds to both climate change and limnological processes. Here the increase in *C. arctica*-type ca 4500–3300 cal yr BP may actually be related to a development of the aquatic mosses at the lake bottom instead not to temperature changes (see Section 4.2.1, Zone Ch-6). Still, we consider this period as a cooling. Actually, the cooling may be underestimated since *C. arctica*-type has higher temperature optimum than other taxa present in the lake in that time interval.

A critical point in our reconstruction is the rather stable late-Holocene temperature reflected in the smoothed as well as the unsmoothed T_{July} curves throughout the past 2500 years (Fig. 5). The remarkable cold events during this period, which are indicated by changes in abundance of cold-stenothermic *P. nivosa*-type from 21 up to 93%, are not reflected in the inferred T_{July} curves. There are several reasons of this phenomenon. First, the studied site with a modern instrumental T_{July} of 4.1 °C is beyond the lower limit of the T_{July} gradient (5.0–18.4 °C) in the Swiss chironomid-temperature calibration data set and the applied chironomid-temperature inference model cannot reconstruct T_{July} cooler than 4 °C. Thus, the chironomid-based reconstruction from SOS fails to track phases of cooler climate in the past. A similar problem also occurred in chironomid-based inferences of the late-Holocene climatic history from the Canadian High Arctic (Axford et al., 2009b). Second, the SOS assemblages with the high relative abundance of *P. nivosa*-type are unusual in the training set (abundance of *Pseudodiamesa* reaches 50% only in one lake), and they have, therefore, a 'very poor' fit to T_{July} (Fig. 7). A 'very poor' fit to temperature may also be related to the low species richness of this high-mountain lake, especially during the late-Holocene, when only two taxa occurred mainly in the chironomid record. Third, the two taxa present in the late-Holocene, *P. nivosa-type* and *M. radialis*-type, are known to be differ in their ecology and distribution along temperature gradients (see Sections 4.1 and 4.2.2). However, since the Swiss training set does not include lakes characterized by a July air temperature lower than 5 °C, they have almost identical temperature WA optima, 7.13 °C and 7.27 °C, respectively. Therefore, any sample comprising only these two taxa gives a similar value of reconstructed temperature irrespective of which taxon is more abundant. Probably, including new lakes from higher altitudes in the calibration data set could provide more accurate estimations of temperature optima for *P. nivosa-type* and *M. radialis*-type and allow inferring cooler temperature.

In addition, Velle et al. (2005, 2010) showed that Holocene temperature inferences from single cores may not always be able to provide a reliable regional temperature signal and should be interpreted with caution. Therefore, in order to obtain a regional picture of Holocene summer temperature change, chironomid-based reconstructions from several sites and inferences from other environmental proxies are needed. Combining different inferred temperature series may reveal the major Holocene temperature patterns.

6. Conclusions

This study provides a high-resolution Holocene sediment record from a remote high-mountain lake, Schwarzsee ob Sölden, and represents the first chironomid-derived palaeotemperature record for the past 10 000 years from the Austrian Alps. At almost 2800 m a.s.l., it is also the highest elevation from which temperatures were reconstructed based on chironomid remains. The PCA ordination suggests that the changes in the chironomid assemblages from this extreme lake were mainly driven by the temperature gradient. A chironomid-temperature transfer function from the Alpine region was applied to the chironomid record. According to the smoothed trend of the temperature inferences, the most significant climatic events at the lake were the early-Holocene thermal maximum (HTM, ca 10 000–8600 cal yr BP) with July air temperatures up to ca 4.5 °C warmer than today, a strong gradual cooling after ca 9200 cal yr BP with a minimum T_{July} ca 3 °C colder than during the HTM at ca 8250–8000 cal yr BP, a long stable and warm mid-Holocene (ca 7900–4500 cal yr BP) with temperatures of ca 6 °C, and a cooling of ca 2 °C during ca 4500–2500 cal yr BP. The Hypsithermal–Neoglaciation transition at ca 5200–4500 cal yr BP is clearly visible in the chironomid record as statistically significant chironomid zone Ch-5. During the late-Holocene (2500–0 cal yr BP), actual mean July temperatures at the lake may have been colder than reconstructed, i.e. below 4 °C, as indicated by high abundances of *P. nivosa*-type. The temperature inferences suggest a warming trend of ca 0.7 °C through the late 20th century at this high-altitude site. Although there were strong fluctuations in the relative abundance of the dominant chironomid species, the last 2500 cal yr BP are the problematic part for quantitative inferences because during this period the studied site has been beyond the temperature range covered by the calibration data set which formed the basis for the applied transfer function.

The climate conditions at Schwarzsee ob Sölden during the Holocene seem to have been largely controlled by orbitally induced insolation changes in the Northern Hemisphere (e.g., the early-Holocene thermal maximum, the Hypsithermal–Neoglaciation transition) and to a lesser extent by variations in the North Atlantic atmospheric and ocean circulation (e.g., the 8.2-ka cold event).

Given that in the Alps the threshold separating the low-altitude and high-altitude thermal regimes of lakes is located at 2000 m a.s.l. during summer (Livingstone et al., 2005), further investigations are needed to gain a calibration data set consisting of high-altitude lakes and to develop a chironomid-based transfer function for summer water temperature. Application of such transfer function to chironomid records from high-altitude lakes, where the main driving force for shifts in limnological variables and biota is climate changes, could help to extract a more reliable regional temperature signal.

Acknowledgements

This research was funded by the Austrian Science Fund (FWF grant M964-N10 to EI and FWF grant R29-N10 to KK). We would like to thank Richard Niederreiter for his help in the coring and Simon Psenner for his assistance in the core processing. We thank Andrea Lami for the analysis of organic carbon, Sophie Kieselbach for the total phosphorus measurements, Ruth Drescher-Schneider for the pollen analysis, Josef Franzoi and Gry Larsen for their assistance in the chemical analyses, and Nikolaus Medgyesy and Dominik Kornthaler for their help during fieldwork 2008. Thanks to Peter Steier, Barbara May, Dietmar Wagenbach, and Andriy Cheburkin for the sediment dating, Denis Scholz for discussion about the age depth model. Reinhard Böhm kindly provided us with information on modern climate conditions at the SOS location. We are grateful to Bo Vinther, Yarrow Axford, and Elena Ortu for making their data available for comparisons. BI has been supported by the European Commission (FP7-PEOPLE-2007-4-2-IIF-ENV Work Programme) via the Marie Curie Fellow project no. 219881. We thank Gaute Velle and an anonymous reviewer for useful comments and suggestions on the original manuscript.

References

ACIA, 2004. Impacts of a Warming Arctic: Arctic Climate Impact Assessment. Cambridge University Press, Cambridge, UK. http://amap.no/acia/.

Adrian, R., O'Reilly, C.M., Zagarese, H., Baines, S.B., Hessen, D.O., Keller, W., Livingstone, D.M., Sommaruga, R., Straile, D., Van Donk, E., Weyhenmeyer, G.A., Winder, M., 2009. Lakes as sentinels of climate change. Limnology and Oceanography 54, 2283–2297.

Alley, R.B., Mayewski, P.A., Sowers, T., Stuiver, M., Taylor, K.C., Clark, P.U., 1997. Holocene climatic instability: a prominent, widespread event 8200 years ago. Geology 25, 483–486.

Alm, T., Willassen, E., 1993. Late Weichselian Chironomidae (Diptera) stratigraphy of Lake Nedre Æråsvatn, Andøya, northern Norway. Hydrobiologia 264, 21–32.

Ambach, W., Blumthaler, M., Wendler, G., 1991. A comparison of ultraviolet radiation measured at an Arctic and an Alpine site. Solar Energy 47, 121–126.

Andreev, A.A., Tarasov, P.E., Ilyashuk, B.P., Ilyashuk, E.A., Cremer, H., Hermichen, W.-D., Wischer, F., Hubberten, H.-W., 2005. Holocene environmental history recorded in the Lake Lyadhej-to sediments, polar Urals, Russia. Palaeogeography, palaeoclimatology, Palaeoecology 223, 181–203.

Armitage, P.D., 1995. Behavior and ecology of adults. In: Armitage, P.D., Cranston, P.S., Pinder, L.C.V. (Eds.), The Chironomidae: Biology and Ecology of Non-biting Midges. Chapman and Hall, London, pp. 194–224.

Auer, I., Böhm, R., Jurkovic, A., Lipa, W., Orlik, A., Potzmann, R., Schöner, W., Ungersbock, M., Matulla, C., Briffa, K., Jones, P., Efthymiadis, D., Brunetti, M., Nanni, T., Maugeri, M., Mercalli, L., Mestre, O., Moisselin, J.M., Begert, M., Müller-Westermeier, G., Kvetov, V., Bochnicek, O., Stastny, P., Lapin, M., Szalai, S., Szentimrey, T., Cegnar, T., Dolinar, M., Gajic-Capkaj, M., Zaninovic, K., Majstorovic, Z., Nieplova, E., 2007. HISTALP – historical instrumental climatological surface time series of the Greater Alpine Region. International Journal of Climatology 27, 17–46.

Axford, Y., Briner, J.P., Cooke, C.A., Francis, D.R., Michelutti, N., Miller, G.H., Smol, J.P., Thomas, E.K., Wilson, C.R., Wolfe, A.P., 2009a. Recent changes in a remote Arctic lake are unique within the past 200,000 years. Proceedings of the National Academy of Sciences of U.S.A. 106, 18443–18446.

Axford, Y., Briner, J.P., Miller, G.H., Francis, D.R., 2009b. Paleoecological evidence for abrupt cold reversals during peak Holocene warmth on Baffin Island, Arctic Canada. Quaternary Research 71, 142–149.

Baroni, C., Orombelli, G., 1996. The alpine 'Iceman' and Holocene climatic change. Quaternary Research 46, 78–83.

Bates, B.C., Kundzewicz, Z.W., Wu, S., Palutikof, J.P., 2008. Climate Change and Water Technical Paper of the Intergovernmental Panel on Climate Change. IPCC Secretariat, Geneva.

Battarbee, R.W., 2000. Palaeolimnological approaches to climate change, with special regard to the biological record. Quaternary Science Reviews 19, 107–124.

Beniston, M., 2005. Mountain climates and climatic change: an overview of Processes focusing on the European Alps. Pure and Applied Geophysics 162, 1587–1606.

Beniston, M., 2006. Mountain weather and climate: a general overview and a focus on climatic changes in the Alps. Hydrobiologia 562, 3–16.

Beniston, M., Jungo, P., 2002. Shifts in the distribution of pressure, temperature and moisture and changes in the typical weather patterns in the Alpine region in response to the behaviour of the North Atlantic Oscillation. Theoretical and Applied Climatilogy 71, 29–42.

Bennett, K.D., 1996. Determination of the number of zones in a biostratigraphical sequence. New Phytologist 132, 155–170.

Bennett, K.D., 2002. Documentation for Psimpoll 4.10 and Pscomb 1.03. C Programs for Plotting Pollen Diagrams and Analyzing Pollen Data. Uppsala University, Uppsala.

Bigler, C., Larocque, I., Peglar, S.M., Birks, H.J.B., Hall, R.I., 2002. Quantitative multiproxy assessment of long-term patterns of Holocene environmental change from a small lake near Abisko, northern Sweden. The Holocene 12, 481–496.

Bigler, C., Heiri, O., Krskova, R., Lotter, A.F., Sturm, M., 2006. Distribution of diatoms, chironomids and cladocera in surface sediments of thirty mountain lakes in southeastern Switzerland. Aquatic Science 68, 154–171.

Birks, H.J.B., 1995. Quantitative palaeoenvironmental reconstructions. In: Maddy, D., Brew, J.S. (Eds.), Statistical Modelling of Quaternary Science Data. Quaternary Research Association, Cambridge, pp. 161–254.

Birks, H.J.B., 1998. Numerical tools in palaeolimnology – progress, potentialities, and problems. Journal of Paleolimnology 20, 307–332.

Birks, H.J.B., Gordon, A.D., 1985. The analysis of pollen stratigraphical data: zonation. In: Birks, H.J.B., Gordon, A.D. (Eds.), Numerical Methods in Quaternary Pollen Analysis. Academic Press, London, pp. 47–90.

Birks, H.J.B., Line, J.M., Juggins, S., Stevenson, A.C., ter Braak, C.J.F., 1990. Diatoms and pH reconstruction. Philosophical Transactions of the Royal Society of London B327, 263–278.

Blumthaler, M., Ambach, W., Ellinger, R., 1997. Increase in solar UV radiation with altitude. Journal of Photochemistry and Photobiology B: Biology 39, 130–134.

Boch, R., Spötl, C., Kramers, J., 2009. High-resolution isotope records of early Holocene rapid climate change from two coeval stalagmites of Katerloch Cave, Austria. Quaternary Science Reviews 28, 2527–2538.

Boggero, A., Füreder, L., Lencioni, V., Simcic, T., Thaler, B., Ferrarese, U., Lotter, A.F., Ettinger, R., 2006. Littoral chironomid communities of Alpine lakes in relation to environmental factors. Hydrobiologia 562, 145–165.

Böhm, R., Auer, I., Brunetti, M., Maugeri, M., Nanni, T., Schöner, W., 2001. Regional temperature variability in the European Alps: 1760–1998 from homogenized instrumental time series. International Journal of Climatology 21, 1779–1801.

Bonani, G., Ivy, S.D., Hajdas, I., Niklaus, T.R., Suter, M., 1994. AMS ^{14}C age determinations of tissue, bone and grass samples from the Ötztal Ice Man. Radiocarbon 36, 247–250.

Booth, R.K., Jackson, S.T., Forman, S.L., Kutzbach, J.E., Bettis III, E.A., Kreig, J., Wright, D.K., 2005. A severe centennial-scale drought in midcontinental North America 4200 years ago and apparent global linkages. The Holocene 15, 321–328.

Bradley, R.S., Keimig, F.T., Diaz, H.F., 2004. Projected temperature changes along the American cordillera and the planned GCOS network. Geophysical Research Letters 31, L16210. doi:10.1029/2004GL020229.

Bretschko, G., 1974. The chironomid fauna of a high-mountain lake (Vorderer Finstertaler See, Tyrol, Austria, 2237 m asl). Entomologisk Tidskrift Supplement 95, 22–33.

Briner, J.P., Michelutti, N., Francis, D.F., Miller, G.H., Axford, Y., Wooller, M.J., Wolfe, A.P., 2006. A multi-proxy lacustrine record of Holocene climate change on northeastern Baffin Island, Arctic Canada. Quaternary Research 65, 431–442.

Bronk, R.C., 2005. OxCal Program, v. 3.10. Radiocarbon Accelerator UNIT. University of Oxford.

Brooks, S.J., Langdon, P.G., Heiri, O., 2007. The Identification and Use of Palaearctic Chironomidae Larvae in Palaeoecology. Quaternary Research Association, London.

Büntgen, U., Esper, J., Frank, D.C., Nicolussi, K., Schmidhalter, M., 2005. A 1052-year tree-ring proxy for Alpine summer temperatures. Climate Dynamics 25, 141–153.

Cleveland, W.S., Grosse, E., Shyu, W.M., 1993. Local regression models. In: Chambers, J.M., Hastie, T.J. (Eds.), Statistical Models in S. Chapman and Hall, London, pp. 309–376.

Corona, C., Guiot, J., Edouard, J.L., Chalié, F., Büntgen, U., Nola, P., Urbinati, C., 2008. Millennium-long summer temperature variations in the European Alps as reconstructed from tree rings. Climate of the Past Discussions 4, 1159–1201.

Crawley, M.J., 1993. GLIM for Ecologists. Blackwell Scientific Publications, Oxford.

Crowley, T.J., 1996. Remembrance of things past: greenhouse lessons from the geologic record. Consequences: the Nature and Implications of Environmental Change 2, 3–12.

Danks, H.V., Oliver, D.R., 1972. Seasonal emergence of some high arctic Chironomidae (Diptera). Canadian Entomologist 104, 661–686.

Efthymiadis, D., Jones, P.D., Briffa, K.R., Auer, I., Bohm, R., Schoner, W., Frei, C., Schmidli, J., 2006. Construction of a 10-Min-Gridded precipitation data set for the Greater alpine region for 1800–2003. Journal of Geophysical Research 111 (D1). doi:10.1029/2005JD006120.

Foley, J.A., Coe, M.T., Scheffer, M., Wang, G., 2003. Regime shifts in the Sahara and Sahel: interactions between ecological and climatic systems in Northern Africa. Ecosystems 6, 524–539.

Grimm, E.C., 2004. TGView Software. Illinois State Museum, Springfield.

Haas, J.N., Richoz, I., Tinner, W., Wick, L., 1998. Synchronous Holocene climate oscillations recorded on the Swiss Plateau and at timberline in the Alps. The Holocene 8, 301–309.

Hågvar, S., Østbye, E., 1973. Notes on some winter-active Chironomidae. Norsk Entomologisk Tidsskrift 20, 253–257.

Heegaard, E., Birks, H.J.B., Telford, R.J., 2005. Relationships between calibrated ages and depth in stratigraphical sequences: an estimation procedure by mixed-effect regression. The Holocene 15, 612–618.

Heiri, O., Lotter, A.F., 2001. Effect of low counts sums on quantitative environmental reconstructions: an example using subfossil chironomids. Journal of Paleolimnology 26, 343–350.

Heiri, O., Lotter, A.F., 2005. Holocene and Lateglacial summer temperature reconstruction in the Swiss Alps based on fossil assemblages of aquatic organisms: a review. Boreas 34, 506–516.

Heiri, O., Lotter, A.F., 2008. Chironomidae (Diptera) in Alpine lakes in Switzerland: a study based on subfossil assemblages in lake surface sediments. Boletim do Museu Municipal do Funchal. Supplement 13, 177–184.

Heiri, O., Lotter, A.F., Hausmann, S., Kienast, F., 2003. A chironomid-based Holocene summer air temperature reconstruction from the Swiss Alps. The Holocene 13, 477–484.

Heiri, O., Cremer, H., Engels, S., Hoek, W.Z., Peeters, W., Lotter, A.F., 2007a. Lateglacial summer temperatures in the Northwest European lowlands: a chironomid record from Hijkermeer, the Netherlands. Quaternary Science Reviews 26, 2420–2437.

Heiri, O., Filippi, M.L., Lotter, A.F., 2007b. Lateglacial summer temperature in the Trentino area (Northern Italy) as reconstructed by fossil chironomid assemblages in Lago di Lavarone (1100 m a.s.l.). Studi Trentini di Scienze Naturali Acta Geologica 82 (2005), 299–308.

Hill, M.O., 1973. Diversity and evenness: a unifying notation and its consequences. Ecology 54, 427–432.

Hormes, A., Beer, J., Schlüchter, C., 2006. A geochronological approach to understanding the role of solar activity on Holocene glacier length variability in the Swiss Alps. Geografiska Annaler 88A, 281–294.

Huber, K., Weckström, K., Drescher-Schneider, R., Knoll, J., Schmidt, J., Schmidt, R., 2010. Climate changes during the last glacial termination inferred from diatom-based temperatures and pollen in a sediment core from Längsee (Austria). Journal of Paleolimnology 43, 131–147.

Ilyashuk, B.P., 2002. Growth and production of aquatic mosses in acidified lakes of Karelia Republic, Russia. Water, Air, and Soil Pollution 135, 285–290.

Ilyashuk, E.A., Ilyashuk, B.P., Hammarlund, D., Larocque, I., 2005. Holocene climatic and environmental changes inferred from midge records (Diptera: Chironomidae, Chaoboridae, Ceratopogonidae) at Lake Berkut, southern Kola Peninsula, Russia. The Holocene 15, 897–914.

Ilyashuk, B., Gobet, E., Heiri, O., Lotter, A.F., van Leeuwen, J.F.N., van der Knaap, W.O., Ilyashuk, E., Oberli, F., Ammann, B., 2009. Lateglacial environmental and

climatic changes at the MalojaPass, Central Swiss Alps, as recorded by chironomids and pollen. Quaternary Science Reviews 28, 1340–1353.
Ilyashuk, B.P., Ilyashuk, E.A., Makarchenko, E.A., Heiri, O., 2010. Midges of the genus *Pseudodiamesa* Goetghebuer (Diptera, Chironomidae): current knowledge and palaeoecological perspective. Journal of Paleolimnology 44, 667–676.
Ivy-Ochs, S., Kerschner, H., Maisch, M., Christl, M., Kubik, P.W., Schlüchter, C., 2009. Latest Pleistocene and Holocene glacier variations in the European Alps. Quaternary Science Reviews 28, 2137–2149.
Joerin, U.E., Stocker, T.F., Schlüchter, C., 2006. Multicentury glacier fluctuations in the Swiss Alps during the Holocene. The Holocene 16, 697–704.
Juggins, S., 2003. C2 User Guide. Software for Ecological and Palaeoecological Data Analysis and Visualisation. University of Newcastle, Newcastle.
Kerschner, H., Hertl, A., Gross, G., Ivy-Ochs, S., Kubik, P.W., 2006. Surface exposure dating of moraines in the Kromer valley (Silvretta Mountains, Austria) – evidence for glacial response to the 8.2 ka event in the Eastern Alps? The Holocene 16, 7–15.
Kobashi, T., Severinghaus, J.P., Brook, E.J., Barnola, J.-M., Grachev, A.M., 2007. Precise timing and characterization of abrupt climate change 8200 years ago from air trapped in polar ice. Quaternary Science Reviews 26, 1212–1222.
Kofler, W., Krapf, V., Oberhuber, W., Bortenschlager, S., 2005. Vegetation responses to the 8200 cal BP cold event and to long-term climatic changes in the Eastern Alps: possible influence of solar activity and North Atlantic freshwater pulses. The Holocene 15, 779–788.
Koinig, K.A., Schmidt, R., Sommaruga-Wögrath, S., Tessadri, R., Psenner, R., 1998. Climate change as the primary cause for pH shifts in a high alpine lake. Water Air and Soil Pollution 104, 167–180.
Koinig, K.A., Ilyashuk, E.A., Tessadri, R., Psenner, R., in preparation. Holocene changes in an alpine lake driven by catchment development, seasonality shifts in insolation and solar activity.
Kröpelin, S., Verschuren, D., Lézine, A.-M., Eggermont, H., Cocquyt, C., Francus, P., Cazet, J.-P., Fagot, M., Rumes, B., Russell, J.M., Darius, F., Conley, D.J., Schuster, M., von Suchodoletz, H., Engstrom, D.R., 2008. Climate-driven ecosystem succession in the Sahara: the past 6000 years. Science 320, 765–768.
Kutzbach, J., Gallimore, R.G., 1988. Sensitivity of a coupled atmosphere and mixed-layer ocean model to changes in orbital forcing at 9000 years BP. Journal of Geophysical Research 93 (D1), 803–821.
Kutzbach, J.E., Webb III, T, 1993. Conceptual basis for understanding Late-Quaternary climates. In: WrightJr, H.E., Kutzbach, J.E., WebbIII, T., Ruddiman, W.F., Street-Perrott, F.A., Bartlein, P.J. (Eds.), Global Climates Since the Last Glacial Maximum. University of Minnesota Press, Minneapolis, pp. 5–11.
Langdon, P.G., Barber, K.E., Lomas-Clarke, S.H., 2004. Reconstructing climate and environmental change in northern England through chironomid and pollen analyses: evidence from Talkin Tarn, Cumbria. Journal of Paleolimnology 32, 197–213.
Langdon, P.G., Leng, M.J., Holmes, N., Caseldine, C.J., 2010. Lacustrine evidence of early-Holocene environmental change in northern Iceland: a multiproxy palaeoecology and stable isotope study. The Holocene 20, 205–214.
Larocque, I., Finsinger, W., 2008. Late-glacial chironomid-based temperature reconstructions for Lago Piccolo di Avigliana in the southwestern Alps (Italy). Palaeogeography, Palaeoclimatology, Palaeoecology 257, 207–223.
Larocque, I., Hall, R.I., Grahn, E., 2001. Chironomids as indicators of climate change: a 100-lake training set from a subarctic region of northern Sweden (Lapland). Journal of Paleolimnology 26, 307–322.
Larocque, I., Grosjean, M., Heiri, O., Bigler, C., Blass, A., 2009. Comparision between chironomid-inferred July temperatures and meteorological data AD 1850–2001 from varved Lake Silvaplana, Switzerland. Journal of Paleolimnology 41, 329–342.
Larocque-Tobler, I., Heiri, O., Wehrli, M., 2010. Lateglacial and Holocene temperature changes at Egelsee, Switzerland, reconstructed using subfossil chironomids. Journal of Paleolimnology 43, 649–666.
Laskar, J., Robutel, P., Joutel, F., Gastineau, M., Correia, A.C.M., Levrard, B., 2004. A long term numerical solution for the insolation quantities of the Earth. Astronomy and Astrophysics 428, 261–285.
Leeman, A., Niessen, F., 1994. Holocene glacial activity and climatic variations in the Swiss Alps: reconstructing a continuous record from pro-glacial lake sediments. The Holocene 4, 259–268.
Legendre, P., Legendre, L., 1998. Numerical Ecology. Elsevier, Amsterdam.
Light, J.J., 1975. Clear lakes and aquatic bryophytes in the mountains of Scotland. Journal of Ecology 63, 937–943.
Livingstone, D.M., Lotter, A.F., Walker, I.R., 1999. The decrease in summer surface water temperature with altitude in Swiss Alpine lakes: a comparison with air temperature lapse rates. Arctic, Antarctic, and Alpine Research 31, 341–352.
Livingstone, D.M., Lotter, A.F., Kettle, H., 2005. Altitude-dependent differences in the primary physical response of mountain lakes to climatic forcing. Limnology and Oceanography 50, 1313–1325.
Lods-Crozet, B., Lencioni, V., Olafsson, J.S., Snook, D.L., Velle, G., Brittain, J.E., Castella, E., Rossaro, B., 2001. Chironomid (Diptera: Chironomidae) communities in six European glacier-fed streams. Freshwater Biology 46, 1791–1809.
Lotter, A.F., Heiri, O., Hofmann, W., van der Knaap, W.O., van Leeuwen, J.F.N., Walker, I.R., Wick, L., 2006. Holocene timber-line dynamics at Bachalpsee, a lake at 2265 m a.s.l. in the northern Swiss Alps. Vegetation History and Archaeobotany 15, 295–307.
MacDonald, G.M., Kremenetski, C.V., Velichko, A.A., Cwynar, L.C., Riding, R.T., Goleva, A.A., Andreev, A.A., Borisova, O.K., Edwards, T.W.D., Hammarlund, D., Szeicz, J.M., Forman, S., Gataullin, V.I., 2000. Holocene treeline history and climate change across Northern Eurasia. Quaternary Research 53, 302–311.
Magny, M., Bégeot, C., 2004. Hydrological changes in the European midlatitudes associated with freshwater outbursts from LakeAgassiz during the Younger Dryas event and the early Holocene. Quaternary Research 61, 181–192.
Magny, M., Haas, J.N., 2004. A major widespread climatic change around 5300 cal yr BP at the time of the Alpine Iceman. Journal of Quaternary Science 19, 423–430.
Magny, M., Guiot, J., Schoellammer, P., 2001. Quantitative reconstruction of Younger Dryas to mid-Holocene paleoclimates at Le Locle, Swiss Jura, using pollen and lake-level data. Quaternary Research 56, 170–180.
Magny, M., Leuzinger, U., Bortenschlager, S., Haas, J.N., 2006. Tripartite climate reversal in Central Europe 5600–5300 years ago. Quaternary Research 65, 3–19.
Mangini, A., Verdes, P., Spötl, C., Scholz, D., Vollweiler, N., Kromer, B., 2007. Persistent influence of the North Atlantic hydrography on central European winter temperature during the last 9000 years. Geophysical Research Letters 34, L02704. doi:10.1029/2006GL028600.
McDermott, F., Frisia, F., Huang, Y., Longinelli, A., Spiro, B., Heaton, T.H.E., Hawkesworth, C.J., Borsato, A., Keppens, E., Fairchild, I.J., van der Borg, K., Verheyden, S., Selmo, E., 1999. Holocene climate variability in Europe: evidence from $d^{18}O$, textural and extension-rate variations in three speleothems. Quaternary Science Reviews 18, 1021–1038.
Millet, L., Arnaud, F., Heiri, O., Magny, M., Verneaux, V., Desmet, M., 2009. Late-Holocene summer temperature reconstruction from chironomid assemblages of Lake Anterne, northern French Alps. The Holocene 19, 317–328.
Milner, A.M., Brittain, J.E., Castella, E., Petts, G.E., 2001. Trends of macro-invertebrate community structure in glacier-fed rivers in relation to environmental conditions: a synthesis. Freshwater Biology 46, 1833–1847.
Nicolussi, K., Patzelt, G., 2000. Discovery of early Holocene wood and peat on the forefield of the Pasterze glacier, Eastern Alps, Austria. The Holocene 10, 191–199.
Nicolussi, K., Patzelt, G., 2001. Untersuchungen zur holozänen Gletscherentwicklung von Pasterze und Gepatschferner (Ostalpen). Zeitschrift für Gletscherkunde und Glazialgeologie 36, 1–87.
Nicolussi, K., Kaufmann, M., Patzelt, G., van der Plicht, J., Thurner, A., 2005. Holocene tree-line variability in the KaunerValley, Central Eastern Alps, indicated by dendrochronological analysis of living trees and subfossil logs. Vegetation History and Archaeobotany 14, 221–234.
Nicolussi, K., Kaufmann, M., Melvin, T.M., van der Plicht, J., Schießling, P., Thurner, A., 2009. A 9111 year long conifer tree-ring chronology for the European Alps: a base for environmental and climatic investigations. The Holocene 19, 909–920.
Oliver, D.R., 1968. Adaptations of arctic Chironomidae. Annales Zoologici Fennici 5, 111–118.
Oliver, D.R., 1971. Life history of the Chironomidae. Annual Review of Entomology 16, 211–230.
Ørbæk, J.B., Tombre, I., Kallenborn, R., 2004. Challenges in arctic-alpine environmental research. Arctic, Antarctic, and Alpine Research 36, 281–283.
Ortu, E., Peyron, O., Bordon, A., de Beaulieu, J.L., Siniscalco, C., Caramiello, R., 2008. Lateglacial and Holocene climate oscillations in the South-western Alps: an attempt at quantitative reconstruction. Quaternary International 190, 71–88.
Parker, B.R., Vinebrooke, R.D., Schindler, D.W., 2008. Recent climate extremes alter alpine lake ecosystems. Proceedings of the National Academy of Sciences of U.S.A. 105, 12927–12931.
Pechlaner, R., Bretschko, G., Gollmann, P., Pfeifer, H., Tilzer, M., Weissenbach, H.E., 1972. The production processes in two high-mountain Lakes (Vorderer and Hinterer Finstertaler See, Kühtai, Austria). In: Kajak, Z., Hillbricht-Ilkowska, A. (Eds.), Proceeding of the IBP-UNESCO Symposium on Productivity Problems of Freshwaters (Kasimierz Dolny, Poland, 1970). Polish Scientific Press, Warsaw, pp. 239–269.
Pinder, L.C.V., 1986. Biology of freshwater Chironomidae. Annual Review of Entomology 31, 1–23.
Raven, P.J., 1988. Occurrence of *Sphagnum* moss in the sublittoral of several small oligotrophic lakes in Galloway, southwest Scotland. Aquatic Botany 30, 223–230.
Reimer, P.J., Baillie, M.G.L., Bard, E., Bayliss, A., Beck, J.W., Bertrand, C.J.H., Blackwell, P.G., Buck, C.E., Burr, G.S., Cutler, K.B., Damon, P.E., Edwards, R.L., Fairbanks, R.G., Friedrich, M., Guilderson, T.P., Hogg, A.G., Hughen, K.A., Kromer, B., McCormac, F.G., Manning, S.W., Ramsey, C.B., Reimer, R.W., Remmele, S., Southon, J.R., Stuiver, M., Talamo, S., Taylor, F.W., van der Plicht, J., Weyhenmeyer, C.E., 2004. IntCal04 Terrestrial radiocarbon age calibration, 26–0 ka BP. Radiocarbon 46, 1029–1058.
Renssen, H., Seppä, H., Heiri, O., Roche, D.M., Goosse, H., Fichefet, T., 2009. The spatial and temporal complexity of the Holocene thermal maximum. Nature Geoscience 2, 411–414.
Rieradevall, M., Bonada, N., Prat, N., 1999. Substrate and depth preferences of macroinvertebrates along a transect in a Pyrenean high mountain lake (Lake Redó, NE Spain). Limnetica 17, 127–134.
Schmidt, R., Kamenik, C., Tessadri, R., Koinig, K.A., 2006. Climatic changes from 12,000 to 4,000 years ago in the Austrian Central Alps tracked by sedimentological and biological proxies of a lake sediment core. Journal of Paleolimnology 35, 491–505.
Schmidt, R., Kamenik, C., Roth, M., 2007. Siliceous algae-based seasonal temperature inferences and indicator pollen tracking 4,000 years of climate/land-use interactions in the southern Austrian Alps. Journal of Paleolimnology 38, 541–554.
Sommaruga-Wögrath, S., Koinig, K.A., Schmidt, R., Sommaruga, R., Tessadri, R., Psenner, R., 1997. Temperature effects on the acidity of remote alpine lakes. Nature 387, 64–67.
Tátosová, J., Stuchlík, E., 2006. Seasonal dynamics of Chironomids in the profundal zone of a Mountain Lake (Ľadové Pleso, the Tatra Mountains, Slovakia). Biologia, Bratislava 61, 203–212.

ter Braak, C.J.F., Juggins, S., 1993. Weighted averaging partial least squares regression (WA-PLS): an improved method for reconstructing environmental variables from species assemblages. Hydrobiologia 269/270, 485–502.
ter Braak, C.J.F., Šmilauer, P., 2002. CANOCO Reference Manual and CanoDraw for Windows User's Quite: Software for Canonical Community Ordination (Version 4.5). Microcomputer Power, New York.
Thies, H., Nickus, U., Mair, V., Tessadri, R., Tait, D., Thaler, B., Psenner, R., 2007. Unexpected response of high alpine lake waters to climate warming. Environmental Science and Technology 41, 7424–7429.
Thompson, R., Kamenik, C., Schmidt, R., 2005. Ultra-sensitive Alpine lakes and climate change. Journal of Limnology 64, 139–152.
Tinner, W., 2007. Treeline studies. In: Elias, S.A. (Ed.), Encyclopedia of Quaternary Science. Elsevier, Amsterdam, pp. 2374–2384.
Tinner, W., Ammann, B., 2001. Timberline paleoecology in the Alps. PAGES News 9/3, 9–11.
Tinner, W., Lotter, A.F., 2001. Central European vegetation response to abrupt climate change at 8.2 ka. Geology 29, 551–554.
Tinner, W., Theurillat, J.P., 2003. Uppermost, limit, extent, and fluctuations of the timberline and tree-line ecotone in the Swiss Central Alps during the past 11500 years. Arctic, Antarctic, and Alpine Research 35, 169–258.
Toivonen, H., Huttunen, P., 1995. Aquatic macrophytes and ecological gradients in 57 small lakes in southern Finland. Aquatic Botany 51, 197–221.
Velichko, A.A., Andreev, A.A., Klimanov, V.A., 1997. The dynamics of climate and vegetation in the tundra and forest zone during the lateglacial and Holocene. Quaternary International 41/42, 71–96.
Velle, G., Brooks, S.J., Birks, H.J.B., Willassen, E., 2005. Chironomids as a tool for inferring Holocene climate: an assessment based on six sites in southern Scandinavia. Quaternary Science Reviews 24, 1429–1462.
Velle, G., Brodersen, K.P., Birks, H.J.B., Willassen, E., 2010. Midges as quantitative temperature indicator species: lessons for palaeoecology. The Holocene 20, 989–1002.
Vinther, B.M., Buchardt, S.L., Clausen, H.B., Dahl-Jensen, D., Johnsen, S.J., Fisher, D.A., Koerner, R.M., Raynaud, D., Lipenkov, V., Andersen, K.K., Blunier, T., Rasmussen, S.O., Steffensen, J.P., Svensson, A.M., 2009. Holocene thinning of the Greenland ice sheet. Nature 461, 385–388.
Vogler, P., 1965. Probleme der Phosphoranalytik in der Limnologie und ein neues Verfahren zur Bestimmung von Orthophosphat neben kondensierten Phosphaten und organischen Phosphorsäureestern. Internationale Revue der gesamten Hydrobiologie 50, 33–48.
Vollweiler, N., Scholz, D., Mühlinghaus, C., Mangini, A., Spötl, C., 2006. A precisely dated climate record for the last 9 kyr from three high alpine stalagmites, Spannagel Cave, Austria. Geophysical Research Letters 33, L20703. doi:10.1029/2006GL027662.
Volpers, M., Neumann, D., 2005. Tolerance of two tubificid species (*Tubifex tubifex* and *Limnodrilus hoffmeisteri*) to hypoxic and sulfidic conditions in novel, long-term experiments. Archiv für Hydrobiologie 164, 13–38.
von Grafenstein, U., Erlenkeuser, H., Müller, J., Jouzel, J., Johnsen, S., 1998. The cold event 8200 years ago documented in oxygen isotope records of precipitation in Europe and Greenland. Climate Dynamics 14, 73–81.
von Gunten, L., Heiri, O., Bigler, C., van Leeuwen, J., Casty, C., Lotter, A.F., Sturm, M., 2008. Seasonal temperatures for the past ~400 years reconstructed from diatom and chironomid assemblages in a high-altitude lake (Lej da la Tscheppa, Switzerland). Journal of Paleolimnology 39, 283–299.
Walker, I.R., 1995. Chironomids as indicators of past environmental change. In: Armitage, P.D., Cranston, P.S., Pinder, L.C.V. (Eds.), The Chironomidae: Biology and Ecology of Non-Biting Midges. Chapman and Hall, London, pp. 405–422.
Walker, I.R., 2001. Midges: Chironomidae and related Diptera. In: Smol, J.P., Birks, H.J.B., Last, W.M. (Eds.), Tracking Environmental Change Using Lake Sediments: Zoological Indicators, vol. 4. Kluwer Academic Publisher, Dordrecht, pp. 43–66.
Wehrli, M., Tinner, W., Ammann, B., 2007. 16,000 years of vegetation and settlement history from Egelsee (Menzingen, Central Switzerland). The Holocene 17, 747–761.
Wiederholm, T. (Ed.), 1983. Chironomidae of the Holarctic Region, Keys and Diagnoses. Part 1 – Larvae. Entomologica Scandinavica, Supplement, vol. 19, pp. 1–457.